

- suva. 2002. Amino acid substitutions in Gag protein at non-cleavage sites are indispensable for the development of a high multitude of HIV-1 resistance against protease inhibitors. *J. Biol. Chem.* 277:5952–5961.
13. Ghosh, A. K., and J. H. Kim. 2004. Stereoselective chloroacetate aldol reactions: syntheses of acetate aldol equivalents and darzens glycidic esters. *Org. Lett.* 6:2725–2728.
 14. Ghosh, A. K., J. F. Kincaid, W. Cho, D. E. Walters, K. Krishnan, K. A. Hussain, Y. Koo, H. Cho, C. Rudall, L. Holland, and J. Buthod. 1998. Potent HIV protease inhibitors incorporating high-affinity P2-ligands and (R)-(hydroxyethylamino)sulfonamide isostere. *Bioorg. Med. Chem. Lett.* 8:687–690.
 15. Ghosh, A. K., K. Krishnan, D. E. Walters, W. Cho, H. Cho, Y. Koo, J. Trevino, L. Holland, and J. Buthod. 1998. Structure based design: novel spirocyclic ethers as nonpeptidic P2-ligands for HIV protease inhibitors. *Bioorg. Med. Chem. Lett.* 8:979–982.
 16. Ghosh, A. K., S. Kulkarni, D. D. Anderson, L. Hong, A. Baldrige, Y. F. Wang, A. A. Chumanovich, A. Y. Kovalevsky, Y. Tojo, M. Amano, Y. Koh, J. Tang, I. T. Weber, and H. Mitsuya. 2009. Design, synthesis, protein-ligand X-ray structure, and biological evaluation of a series of novel macrocyclic human immunodeficiency virus-1 protease inhibitors to combat drug resistance. *J. Med. Chem.* 52:7689–7705.
 17. Ghosh, A. K., S. Leshchenko, and M. Noetzel. 2004. Stereoselective photochemical 1,3-dioxolane addition to 5-alkoxymethyl-2(5H)-furanone: synthesis of bis-tetrahydrofuran ligand for HIV protease inhibitor UIC-94017 (TMC-114). *J. Org. Chem.* 69:7822–7829.
 18. Girouard, M., K. Diallo, B. Marchand, S. McCormick, and M. Gotte. 2003. Mutations E44D and V118I in the reverse transcriptase of HIV-1 play distinct mechanistic roles in dual resistance to AZT and 3TC. *J. Biol. Chem.* 278:34403–34410.
 19. Gotte, M., D. Arion, M. A. Parniak, and M. A. Wainberg. 2000. The M184V mutation in the reverse transcriptase of human immunodeficiency virus type 1 impairs rescue of chain-terminated DNA synthesis. *J. Virol.* 74:3579–3585.
 20. Gupta, R., A. Hill, A. W. Sawyer, and D. Pillay. 2008. Emergence of drug resistance in HIV type 1-infected patients after receipt of first-line highly active antiretroviral therapy: a systematic review of clinical trials. *Clin. Infect. Dis.* 47:712–722.
 21. Hog, R. 2008. Life expectancy of individuals on combination antiretroviral therapy in high-income countries: a collaborative analysis of 14 cohort studies. *Lancet* 372:293–299.
 22. Koh, Y., D. Das, S. Leschenko, H. Nakata, H. Ogata-Aoki, M. Amano, M. Nakayama, A. K. Ghosh, and H. Mitsuya. 2009. GRL-02031, a novel non-peptidic protease inhibitor (PI) containing a stereochemically defined fused cyclopentanyltetrahydrofuran potent against multi-PI-resistant human immunodeficiency virus type 1 in vitro. *Antimicrob. Agents Chemother.* 53:997–1006.
 23. Koh, Y., S. Matsumi, D. Das, M. Amano, D. A. Davis, J. Li, S. Leschenko, A. Baldrige, T. Shioda, R. Yarchoan, A. K. Ghosh, and H. Mitsuya. 2007. Potent inhibition of HIV-1 replication by novel non-peptidyl small molecule inhibitors of protease dimerization. *J. Biol. Chem.* 282:28709–28720.
 24. Koh, Y., H. Nakata, K. Maeda, H. Ogata, G. Bilcer, T. Devasamudram, J. F. Kincaid, P. Boross, Y. F. Wang, Y. Tie, P. Volarath, L. Gaddis, R. W. Harrison, I. T. Weber, A. K. Ghosh, and H. Mitsuya. 2003. Novel bis-tetrahydrofuranyluethane-containing nonpeptidic protease inhibitor (PI) UIC-94017 (TMC114) with potent activity against multi-PI-resistant human immunodeficiency virus in vitro. *Antimicrob. Agents Chemother.* 47:3123–3129.
 25. Kovalevsky, A. Y., A. K. Ghosh, and I. T. Weber. 2008. Solution kinetics measurements suggest HIV-1 protease has two binding sites for darunavir and amprenavir. *J. Med. Chem.* 51:6599–6603.
 26. Larder, B. A., S. D. Kemp, and P. R. Harrigan. 1995. Potential mechanism for sustained antiretroviral efficacy of AZT-3TC combination therapy. *Science* 269:696–699.
 27. Little, S. J., S. Holte, J. P. Routy, E. S. Daar, M. Markowitz, A. C. Collier, R. A. Koup, J. W. Mellors, E. Connick, B. Conway, M. Kilby, L. Wang, J. M. Whitcomb, N. S. Hellmann, and D. D. Richman. 2002. Antiretroviral-drug resistance among patients recently infected with HIV. *N. Engl. J. Med.* 347:385–394.
 28. Maeda, K., K. Yoshimura, S. Shibayama, H. Habashita, H. Tada, K. Sagawa, T. Miyakawa, M. Aoki, D. Fukushima, and H. Mitsuya. 2001. Novel low molecular weight spirodiketopiperazine derivatives potently inhibit R5 HIV-1 infection through their antagonistic effects on CCR5. *J. Biol. Chem.* 276:35194–35200.
 29. Mitsuya, H., and J. Erickson. 1999. Discovery and development of antiretroviral therapeutics for HIV infection, p. 751–780. *In* T. C. Merigan, J. G. Bartlett, and D. Bolognesi (ed.), *Textbook of AIDS medicine*. The Williams & Wilkins Co., Baltimore, MD.
 30. Murphy, E. L., A. C. Collier, L. A. Kalish, S. F. Assmann, M. F. Para, T. P. Flanagan, P. N. Kumar, L. Mintz, F. R. Wallach, and G. J. Nemo. 2001. Highly active antiretroviral therapy decreases mortality and morbidity in patients with advanced HIV disease. *Ann. Intern. Med.* 135:17–26.
 31. Naeger, L. K., and K. A. Struble. 2007. Food and Drug Administration analysis of tipranavir clinical resistance in HIV-1-infected treatment-experienced patients. *AIDS* 21:179–185.
 32. Shirasaka, T., R. Yarchoan, M. C. O'Brien, R. N. Husson, B. D. Anderson, E. Kojima, T. Shimada, S. Broder, and H. Mitsuya. 1993. Changes in drug sensitivity of human immunodeficiency virus type 1 during therapy with azidothymidine, dideoxycytidine, and dideoxyinosine: an in vitro comparative study. *Proc. Natl. Acad. Sci. U. S. A.* 90:562–566.
 33. Siliciano, J. D., and R. F. Siliciano. 2004. A long-term latent reservoir for HIV-1: discovery and clinical implications. *J. Antimicrob. Chemother.* 54:6–9.
 34. Tie, Y., P. I. Boross, Y. F. Wang, L. Gaddis, A. K. Hussain, S. Leshchenko, A. K. Ghosh, J. M. Louis, R. W. Harrison, and I. T. Weber. 2004. High resolution crystal structures of HIV-1 protease with a potent non-peptide inhibitor (UIC-94017) active against multi-drug-resistant clinical strains. *J. Mol. Biol.* 338:341–352.
 35. Walensky, R. P., A. D. Paltiel, E. Losina, L. M. Mercincavage, B. R. Schackman, P. E. Sax, M. C. Weinstein, and K. A. Freedberg. 2006. The survival benefits of AIDS treatment in the United States. *J. Infect. Dis.* 194:11–19.
 36. Yoshimura, K., R. Kato, M. F. Kavlick, A. Nguyen, V. Maroun, K. Maeda, K. A. Hussain, A. K. Ghosh, S. V. Gulnik, J. W. Erickson, and H. Mitsuya. 2002. A potent human immunodeficiency virus type 1 protease inhibitor, UIC-94003 (TMC-126), and selection of a novel (A28S) mutation in the protease active site. *J. Virol.* 76:1349–1358.
 37. Yoshimura, K., R. Kato, K. Yusa, M. F. Kavlick, V. Maroun, A. Nguyen, T. Mimoto, T. Ueno, M. Shintani, J. Falloon, H. Masur, H. Hayashi, J. Erickson, and H. Mitsuya. 1999. JE-2147: a dipeptide protease inhibitor (PI) that potently inhibits multi-PI-resistant HIV-1. *Proc. Natl. Acad. Sci. U. S. A.* 96:8675–8680.



Synthesis and biological evaluation of novel allophenylnorstatine-based HIV-1 protease inhibitors incorporating high affinity P2-ligands

Arun K. Ghosh^{a,*}, Sandra Gemma^a, Elena Simoni^a, Abigail Baldrige^a, D. Eric Walters^b, Kazuhiko Ide^c, Yasushi Tojo^c, Yasuhiro Koh^c, Masayuki Amano^c, Hiroaki Mitsuya^{c,d}

^a Departments of Chemistry and Medicinal Chemistry, Purdue University, West Lafayette, IN 47907, United States

^b Departments of Biochemistry and Molecular Biology, Rosalind Franklin University of Medicine and Science, North Chicago, IL 60064, United States

^c Departments of Hematology and Infectious Diseases, Kumamoto University School of Medicine, Kumamoto 860-8556, Japan

^d Experimental Retrovirology Section, HIV and AIDS Malignancy Branch, National Cancer Institute, Bethesda, MD 20892, United States

ARTICLE INFO

Article history:

Received 19 October 2009

Revised 20 November 2009

Accepted 23 November 2009

Available online 5 December 2009

Keywords:

HIV protease

Inhibitors

Darunavir

Allophenylnorstatine

Design

Synthesis

ABSTRACT

A series of stereochemically defined cyclic ethers as P2-ligands were incorporated in an allophenylnorstatine-based isostere to provide a new series of HIV-1 protease inhibitors. Inhibitors **3b** and **3c**, containing conformationally constrained cyclic ethers, displayed impressive enzymatic and antiviral properties and represent promising lead compounds for further optimization.

© 2009 Elsevier Ltd. All rights reserved.

The introduction of protease inhibitors into highly active anti-retroviral treatment (HAART) regimens with reverse transcriptase inhibitors represented a major breakthrough in AIDS chemotherapy.¹ This combination therapy has significantly increased life expectancy, and greatly improved the course of HIV management. Therapeutic inhibition of HIV-1 protease leads to morphologically immature and noninfectious viral particles.² However, under the selective pressure of chemotherapeutics, rapid adaptation of viral enzymes generates strains resistant to one or more antiviral agents.³ As a consequence, a growing number of HIV/AIDS patients harbor multidrug-resistant HIV strains. There is ample evidence that such strains can be readily transmitted.⁴ Therefore, one of the major current therapeutic objectives has been to develop novel protease inhibitors (PIs) with broad-spectrum activity against multidrug-resistant HIV-1 variants. In our continuing interest in developing concepts and strategies to combat drug-resistance, we have reported a series of novel PIs including Darunavir, TMC-126, GRL-06579, and GRL-02031.^{5–8} These inhibitors have shown exceedingly potent enzyme inhibitory and antiviral activity as well as exceptional broad spectrum activity against highly cross-resistant mutants. Darunavir, which incorporates a (*R*)-(hydroxymethyl)-sulfonamide isostere and a stereochemically defined bis-tetrahy-

drofuran (bis-THF) as the P2-ligand, was initially approved for the treatment of patients with drug-resistant HIV and more recently, it has been approved for all HIV/AIDS patients including pediatrics⁹ (Fig. 1).

Darunavir was designed based upon the 'backbone binding' concept developed in our laboratories. Darunavir-bound X-ray structure revealed extensive hydrogen bonding with the protease backbone throughout the enzyme active site.¹⁰ The P2-bis-THF ligand is responsible for its superior drug-resistance properties. The bis-THF ligand has been documented as a privileged ligand for the S2-subsite. Incorporation of this ligand into other transition-state isosteres also resulted in significant potency enhancement.¹¹ Besides 3(*S*)-THF, and [3*aS*,5*S*,6*R*]-bis-THF, we have designed a number of other novel cyclic ether-based high affinity ligands. Incorporation of these ligands in (*R*)-(hydroxyethyl)-sulfonamide isosteres provided PIs with excellent potency and drug-resistance properties.^{6–8} We then investigated the potential of these structure-based designed P2-ligands in a KNI-764-derived isostere designed by Mimoto and co-workers.¹² This PI incorporates an allophenylnorstatine isostere. Interestingly, KNI-764 has maintained good activity against HIV-1 clinical strains resistant to several FDA-approved PIs. The flexible *N*-(2-methyl benzyl) amide P2'-ligand may have been responsible for its activity against drug-resistant HIV-1 strains as the flexible chain allows better adaptability to mutations.^{12,13} The bis-THF and other structure-based designed P2-ligands, make several critical

* Corresponding author. Tel.: +1 765 494 5323; fax: +1 765 496 1612.
E-mail address: akghosh@purdue.edu (A.K. Ghosh).

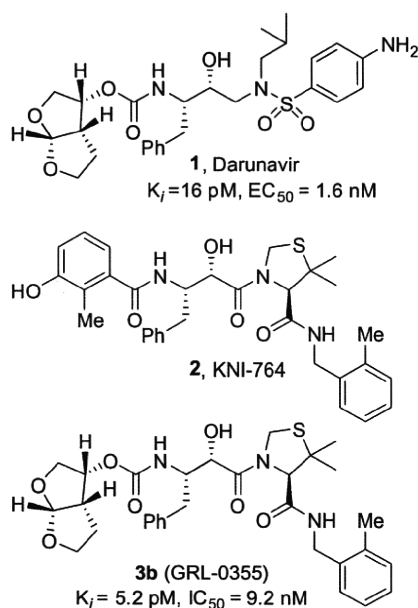
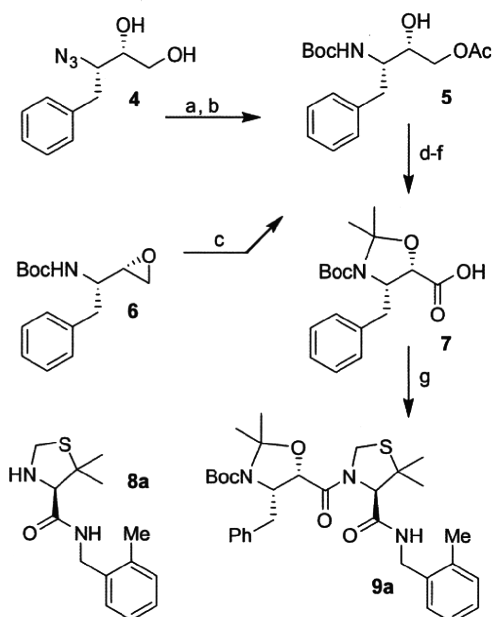


Figure 1. Structures of inhibitors 1, 2, and 3b.

hydrogen bonds with the protein backbone, particularly with Asp-29 and Asp-30 NH's.¹¹ Therefore, incorporation of these ligands into the KNI-764-derived isostere, may lead to novel PIs with improved potency and efficacy against multidrug-resistant HIV-1 variants. Furthermore, substitution of the P2-phenolic derivative in KNI-764 with a cyclic ether-based ligand could result in improved metabolic stability and pharmacological properties since phenol glucuronide is readily formed when KNI-764 is exposed to human hepatocytes in vitro.¹²

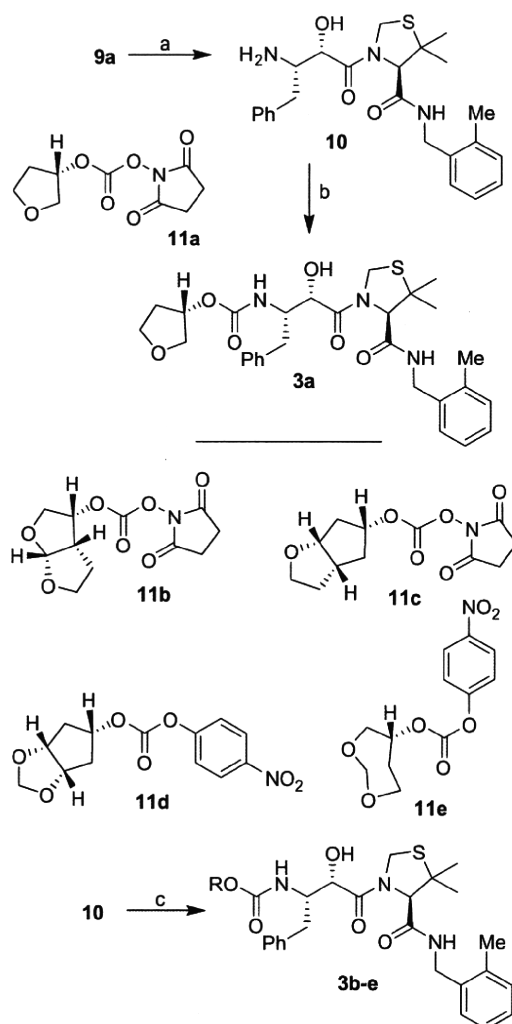
The synthesis of target compounds **3a–e** was accomplished as described in Scheme 1. Our synthetic plan for carboxylic acid **7** (Scheme 1) involved the preparation of the key intermediate **5** through two different synthetic pathways. In the first approach,



Scheme 1. Reagents: (a) H_2 , Pd/C, Boc_2O , EtOAc; (b) Ac_2O , Pyr, DMAP; (c) $LiCO_3$, AcOH, DMF; (d) 2-methoxypropene, CSA, DCM; (e) K_2CO_3 , MeOH; (f) $RuCl_3$, $NaIO_4$, CCl_4 -MeCN- H_2O (2:2:3); (g) *N*-methylmorpholine, $iBuOCOC$, **8a**, THF.

known optically active azidodiol **4**¹⁴ was first hydrogenated in the presence of Boc_2O . The resulting diol was converted to **5** by selective acylation of the primary alcohol with acetic anhydride in the presence of pyridine and a catalytic amount of DMAP at $0^\circ C$ for 4 h to provide **5** in 77% overall yield. As an alternative approach, commercially available optically active epoxide **6** was exposed to lithium acetate, formed in situ from lithium carbonate and acetic acid in DMF. This resulted in the regioselective opening¹⁵ of the epoxide ring and afforded compound **5** in 62% yield. The alcohol **5** thus obtained was protected as the corresponding acetone by treatment with 2-methoxypropene in the presence of a catalytic amount of CSA. The acetate group was subsequently hydrolyzed in the presence of potassium carbonate in methanol to afford the corresponding alcohol. This was subjected to an oxidation reaction using ruthenium chloride hydrate and sodium periodate in a mixture of aqueous acetonitrile and CCl_4 at $23^\circ C$ for 10 h. This resulted in the formation of the target carboxylic acid **7** in 61% yield. Amide **9a** was prepared by activation of carboxylic acid **7** into the corresponding mixed anhydride by treatment with isobutylchloroformate followed by reaction with amine **8a**.^{16,17}

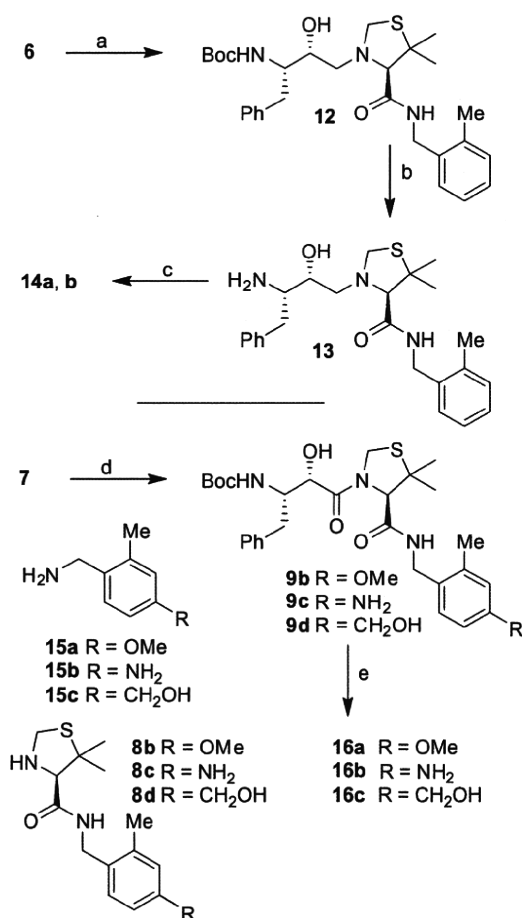
Synthesis of various inhibitors was carried out as shown in Scheme 2. Deprotection of the Boc and acetone groups was carried out by exposure of **9** to a 1 M solution of hydrochloric acid in methanol at $23^\circ C$ for 8 h. This provided amine **10** in quantitative



Scheme 2. Reagents: (a) 1 M HCl, MeOH; (b) **11a**, Et_3N , CH_2Cl_2 ; (c) **11b,c**, Et_3N , CH_2Cl_2 ; or, **11d,e**, DIPEA, THF.

yield. Reaction of **11a** with amine **10** in CH_2Cl_2 in the presence of Et_3N at 23°C for 6 h, provided inhibitor **3a** in 62% yield. The 3(*S*)-tetrahydrofuran-2-yl carbonate **11a** was prepared as described previously.¹⁸ Similarly, allophenylnorstatine-based inhibitors **3b–e** were synthesized. As shown, carbonates **11b**,¹⁹ **11c**,⁷ and **11d–e**¹⁹ were prepared as previously described. Reaction of these carbonates with amine **10** furnished the desired inhibitors **3b–e** in 45–62% yield.

The syntheses of inhibitors **14a,b** and **16a–c** were carried out as shown in Scheme 3. Inhibitors **14a,b**, containing hydroxyethylamine isostere were prepared by opening epoxide **6** with amine **8a** in the presence of lithium perchlorate in diethyl ether at 23°C for 5 h to provide amino alcohol **12** in 64% yield. Removal of the Boc-group by exposure to 1 M HCl in MeOH at 23°C for 12 h afforded amine **13**. Reactions of amine **13** with activated carbonates **11a** and **11b** afforded urethane **14a** and **14b** in 44% and 59% yields, respectively. For the synthesis of inhibitors **16a–c**, commercially available (*R*)-5,5-dimethyl-thiazolidine-4-carboxylic acid was protected as its Boc-derivative. The resulting acid was coupled with amines **15a–c** in the presence of DCC and DMAP in CH_2Cl_2 to provide the corresponding amides. Removal of the Boc-group by exposure to 30% trifluoroacetic acid afforded **8b–d**. Coupling of these amines with acid **7** as described in Scheme 1, provided the corresponding products **9b–d**. Removal of Boc-group and reactions of the resulting amines with activated carbonate **11b** furnished inhibitors **16a–c** in good yields (55–60%).



Scheme 3. Reagents: (a) **8a**, $\text{Li}(\text{ClO}_4)$, Et_2O ; (b) $\text{CF}_3\text{CO}_2\text{H}$, CH_2Cl_2 ; (c) **11a** or **11b**, Et_3N , CH_2Cl_2 ; (d) *N*-methylmorpholine, isobutylchloroformate, **8b–d**, THF; (e) $\text{CF}_3\text{CO}_2\text{H}$, CH_2Cl_2 , then **11b**, Et_3N , CH_2Cl_2 .

Inhibitors **3a–e** were first evaluated in enzyme inhibitory assay utilizing the protocol described by Toth and Marshall.²⁰ Compounds that showed potent enzymatic K_i values were then further evaluated in antiviral assay. The inhibitor structure and potency are shown in Table 1. As shown, incorporation of a stereochemically defined 3(*S*)-tetrahydrofuran ring as the P2-ligand provided inhibitor **3a**, which displayed an enzyme inhibitory potency of 0.2 nM and antiviral IC_{50} value of 20 nM. The corresponding derivative **14a** with a hydroxyethylamine isostere exhibited over 400-fold reduction in enzyme inhibitory activity. Introduction of a stereochemically defined bis-THF as the P2-ligand, resulted in inhibitor **3b**, which displayed over 40-fold potency enhancement with respect to **3a**. Inhibitor **3b** displayed a K_i of 5.2 pM in the enzyme inhibitory assay. Furthermore, compound **3b** has shown an impressive antiviral activity with an IC_{50} value of 9 nM. Inhibitor **14b** with hydroxyethylamine isostere is significantly less potent than the corresponding norstatine-derived inhibitor **3b**. Inhibitor **3c** with a (3*aS*, 5*R*, 6*aR*)-5-hydroxy-hexahydrocyclopenta[*b*]furan as the P2-ligand has displayed excellent inhibitory activity, and particularly, antiviral activity, showing an IC_{50} value of 13 nM. Other structure-based designed ligands in inhibitors **3d** and **3e** have shown subnanomolar enzyme inhibitory activity. However, inhibitor **3b** with a bis-THF ligand has shown the most impressive activity.

To obtain molecular insight into the possible ligand-binding site interactions, we have created energy-minimized models of a number of inhibitors based upon protein-ligand X-ray structure of KNI-764 (**2**).²¹ An overlayed model of **3b** with the X-ray structure of 2-bound HIV-1 protease is shown in Figure 2. This model for inhibitor **3b** was created from the X-ray crystal structure of KNI-764 (**2**)-bound HIV-1 protease (KNI-764, pdb code 1MSM²¹) and the X-ray crystal structure of darunavir (pdb code 2IEN²²), by combining the P2-end of the darunavir structure with the P2'-end of the KNI-764 structure, followed by 1000 cycles of energy minimization. It appears that both oxygens of the bis-THF ligand are suitably located to form hydrogen bonds with the backbone atoms of Asp-29 and Asp-30 NH's, similar to darunavir-bound HIV-1 protease.¹⁰ Furthermore, the KNI-764-X-ray structure-derived model of **3b** suggested that the incorporation of appropriate substituents on the phenyl ring could interact with Asp-29' and Asp-30' in the S2'-subsite. In particular, it appears that a 4-hydroxymethyl substituent on the P2'-phenyl ring could conceivably interact with backbone Asp-30' NH in the S2'-subsite. Other substituents such as a methoxy group or an amine functionality also appears to be within proximity to Asp-29' and Asp-30' backbone NHs. Based upon these speculations, we incorporated *p*-MeO, *p*-NH₂ and *p*-CH₂OH substituents on the P2'-phenyl ring of inhibitor **3b**. As shown in Table 1, neither *p*-MeO nor *p*-NH₂ groups improved enzyme inhibitory potency compared to inhibitor **3b**. Of particular note, compound **16a**, displayed a good antiviral potency, possibly suggesting a better penetration through the cell membrane. Inhibitor **16c** with a hydroxymethyl substituent showed sub-nanomolar enzyme inhibitory potency but its antiviral activity was moderate compared to unsubstituted derivative **3b**. As it turned out, inhibitor **3b** is the most potent inhibitor in the series. We subsequently examined its activity against a clinical wild-type X₄-HIV-1 isolate (HIV-1_{ERS104pre}) along with various multidrug-resistant clinical X₄- and R₅-HIV-1 isolates using PBMCs as target cells.^{5b} As can be seen in Table 2, the potency of **3b** against HIV-1_{ERS104pre} (IC_{50} = 31 nM) was comparable to the FDA approved PI, amprenavir with an IC_{50} value of 45 nM. Darunavir and atazanavir on the other hand, are significantly more potent with IC_{50} values of 5 nM and 3 nM, respectively. Inhibitor **3b**, while less potent than darunavir, maintained 5-fold or better potency over amprenavir against HIV-1_{MDR/C}, HIV-1_{MDR/G}, HIV-1_{MDR/TM} and HIV-1_{MDR/MM}. It maintained over a 2-fold potency against HIV-1_{MDR/JSL}. In fact, inhibitor **3b** maintained comparable potency to atazanavir against all

Table 1
Enzymatic inhibitory and antiviral activity of allophenylnorstatine-derived inhibitors

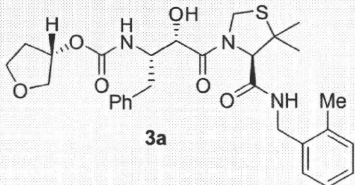
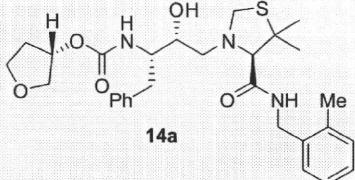
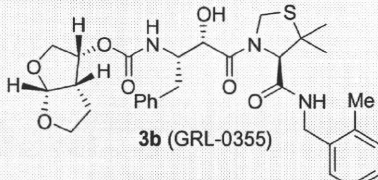
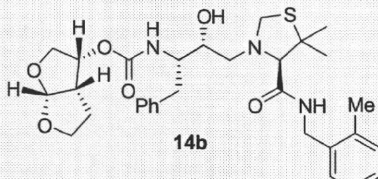
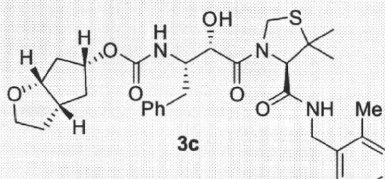
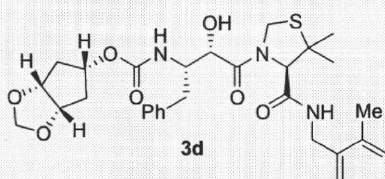
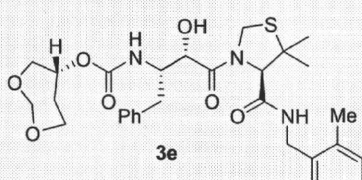
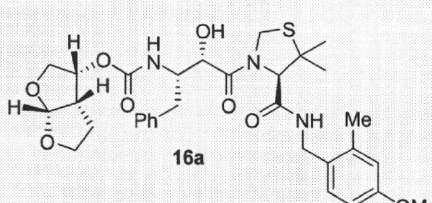
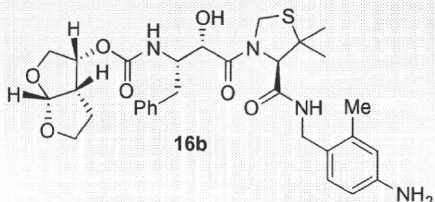
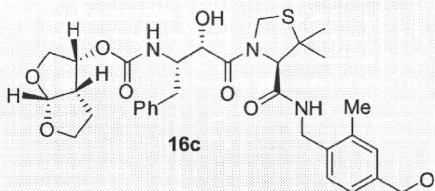
Entry	Inhibitor	K_i (nM)	$IC_{50}^{a,b}$ (μ M)
1	 3a	0.21	0.02
2	 14a	86.2	nt
3	 3b (GRL-0355)	0.0052	0.009
4	 14b	2.6	nt
5	 3c	0.29	0.013
6	 3d	0.65	nt
7	 3e	0.78	nt
8	 16a	2.03	0.051

Table 1 (continued)

Entry	Inhibitor	K_i (nM)	$IC_{50}^{a,b}$ (μ M)
9	 16b	1.01	0.53
10	 16c	0.31	0.23

^a Values are means of at least three experiments.

^b Human lymphoid (MT-2) cells were exposed to 100 TCID₅₀ values of HIV-1_{LA1} and cultured in the presence of each PI, and IC_{50} values were determined using MTT assay. Darunavir exhibited K_i = 16 pM, IC_{50} = 1.6 nM.

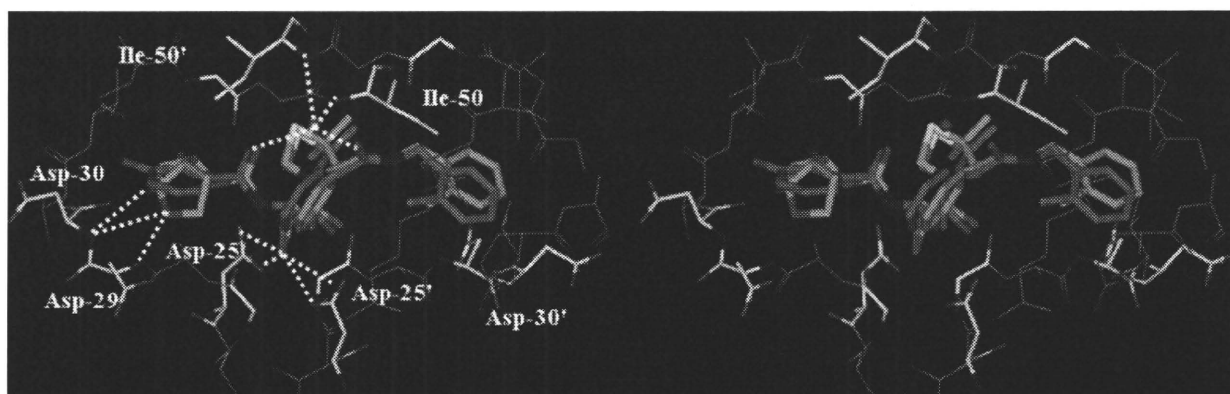


Figure 2. Structure of inhibitor **3b**, modeled into the active site of HIV-1 protease, superimposed on the X-ray crystal structure of KNI-764. Inhibitor **3b** carbons are shown in green and KNI-764 carbons are shown in magenta.

Table 2

Antiviral activity of **3b** (GRL-0355) against multidrug-resistant clinical isolates in PHA-PBMs.

Virus	IC_{50} (μ M)			
	3b (GRL-0355)	APV	ATV	DRV
HIV-1 _{ERS104pre} (wild-type: X4)	0.031 \pm 0.002	0.045 \pm 0.014	0.003 \pm 0.003	0.005 \pm 0.001
HIV-1 _{MDR/C} (X4)	0.061 \pm 0.005 (2)	0.346 \pm 0.071 (8)	0.045 \pm 0.026 (15)	0.010 \pm 0.006 (2)
HIV-1 _{MDR/G} (X4)	0.029 \pm 0.002 (1)	0.392 \pm 0.037 (9)	0.029 \pm 0.020 (10)	0.019 \pm 0.005 (4)
HIV-1 _{MDR/TM} (X4)	0.064 \pm 0.032 (2)	0.406 \pm 0.082 (9)	0.047 \pm 0.009 (16)	0.007 \pm 0.003 (1)
HIV-1 _{MDR/MM} (R5)	0.042 \pm 0.001 (1)	0.313 \pm 0.022 (7)	0.040 \pm 0.002 (13)	0.027 \pm 0.008 (5)
HIV-1 _{MDR/JSI} (R5)	0.235 \pm 0.032 (8)	0.531 \pm 0.069 (12)	0.635 \pm 0.065 (212)	0.028 \pm 0.008 (6)

The amino acid substitutions identified in the protease-encoding region of HIV-1_{ERS104pre}, HIV-1_C, HIV-1_G, HIV-1_{MM}, HIV-1_{JSI} compared to the consensus type B sequence cited from the Los Alamos database include L63P; L10I, I15V, K20R, L24I, M36I, M46L, I54V, I62V, L63P, K70Q, V82A, L89M; L10I, V11I, T12E, I15V, L19I, R41K, M46L, L63P, A71T, V82A, L90M; L10I, K14R, R41K, M46L, I54V, L63P, A71V, V82A, L90M; L10I, K43T, M46L, I54V, L63P, A71V, V82A, L90M, Q92K; and L10I, L24I, I33F, E35D, M36I, N37S, M46L, I54V, R57K, I62V, L63P, A71V, G73S, V82A, respectively. HIV-1_{ERS104pre} served as a source of wild-type HIV-1. The IC_{50} values were determined by using PHA-PBMs as target cells and the inhibition of p24 Gag protein production by each drug was used as an endpoint. The numbers in parentheses represent the fold changes of IC_{50} values for each isolate compared to the IC_{50} values for wild-type HIV-1_{ERS104pre}. All assays were conducted in duplicate, and the data shown represent mean values (\pm 1 standard deviations) derived from the results of two or three independent experiments. Amprenavir = APV; Atazanavir = ATV; Darunavir = DRV.

multidrug-resistant clinical isolates tested. The reason for its impressive potency against multidrug-resistant clinical isolates is possibly due to its ability to make extensive hydrogen-bonds with the protease backbone in the S2 subsite and its ability to fill in the hydrophobic pockets in the S1'–S2' subsites effectively.

In conclusion, incorporation of stereochemically defined and conformationally constrained cyclic ethers into the allophenyl-norstatine resulted in a series of potent protease inhibitors. The promising inhibitors **3b** and **3c** are currently being subjected to further in-depth biological studies. Design and synthesis of new

classes of inhibitors based upon above molecular insight are currently ongoing in our laboratories.

Acknowledgement

The financial support of this work is provided by the National Institute of Health (GM 83356).

References and notes

- Sepkowitz, K. A. *N. Eng. J. Med.* **2001**, *344*, 1764–1772.
- Kohl, N. E.; Emini, E. A.; Schleif, W. A.; Davis, L. J.; Heimbach, J. C.; Dixon, R. A. F.; Scolnick, E. M.; Sigal, I. S. *Proc. Natl. Acad. Sci. U.S.A.* **1988**, *85*, 4686–4690.
- (a) Pillay, D.; Bhaskaran, K.; Jurriaans, S.; Prins, M.; Masquelier, B.; Dabis, F.; Gifford, R.; Nielsen, C.; Pedersen, C.; Balotta, C.; Rezza, G.; Ortiz, M.; de Mendoza, C.; Kücherer, C.; Poggensee, G.; Gill, J.; Porter, K. *AIDS* **2006**, *20*, 21–28; (b) Grabar, S.; Pradier, C.; Le Corfec, E.; Lancar, R.; Allavena, C.; Bentata, M.; Berlureau, P.; Dupont, C.; Fabbro-Peray, P.; Poizot-Martin, I.; Costagliola, D. *AIDS* **2000**, *14*, 141–149.
- Wainberg, M. A.; Friedland, G. *JAMA* **1998**, *279*, 1977–1983.
- (a) Ghosh, A. K.; Kincaid, J. F.; Cho, W.; Walters, D. E.; Krishnan, K.; Hussain, K. A.; Koo, Y.; Cho, H.; Rudall, C.; Holland, L.; Buthod, J. *Bioorg. Med. Chem. Lett.* **1998**, *8*, 687–690; (b) Koh, Y.; Maeda, K.; Ogata, H.; Bilcer, G.; Devasamudram, T.; Kincaid, J. F.; Boross, P.; Wang, Y.-F.; Tie, Y.; Volarath, P.; Gaddis, L.; Louis, J. M.; Harrison, R. W.; Weber, I. T.; Ghosh, A. K.; Mitsuya, H. *Antimicrob. Agents Chemother.* **2003**, *47*, 3123–3129; (c) Ghosh, A. K.; Pretzer, E.; Cho, H.; Hussain, K. A.; Duzgunes, N. *Antiviral Res.* **2002**, *54*, 29–36.
- Yoshimura, K.; Kato, R.; Kavlick, M. F.; Nguyen, A.; Maroun, V.; Maeda, K.; Hussain, K. A.; Ghosh, A. K.; Gulnik, S. V.; Erickson, J. W.; Mitsuya, H. *J. Virol.* **2002**, *76*, 1349–1358.
- Ghosh, A. K.; Sridhar, P. R.; Leshchenko, S.; Hussain, A. K.; Li, J.; Kovalevsky, A. Y.; Walters, D. E.; Wedekind, J. K.; Grum-Tokars, V.; Das, D.; Koh, Y.; Maeda, K.; Gatanaga, H.; Weber, I. T.; Mitsuya, H. *J. Med. Chem.* **2006**, *49*, 5252.
- Koh, Y.; Das, D.; Leshchenko, S.; Nakata, H.; Ogata-Aoki, H.; Amano, M.; Nakayama, M.; Ghosh, A. K.; Mitsuya, H. *Antimicrob. Agents Chemother.* **2009**, *53*, 997–1006.
- (a) FDA approved Darunavir on June 23, 2006: FDA approved new HIV treatment for patients who do not respond to existing drugs. Please see: <http://www.fda.gov/NewsEvents/Newsroom/PressAnnouncements/2006/ucm108676.htm> (b) On October 21, 2008, FDA granted traditional approval to Prezista (darunavir), co-administered with ritonavir and with other antiretroviral agents, for the treatment of HIV-1 infection in treatment-experienced adult patients. In addition to the traditional approval, a new dosing regimen for treatment-naïve patients was approved.
- Ghosh, A. K.; Chapsal, B. D.; Weber, I. T.; Mitsuya, H. *Acc. Chem. Res.* **2008**, *41*, 78–86.
- Ghosh, A. K.; Ramu Sridhar, P.; Kumaragurubaran, N.; Koh, Y.; Weber, I. T.; Mitsuya, H. *ChemMedChem* **2006**, *1*, 939–950.
- Mimoto, T.; Terashima, K.; Nojima, S.; Takaku, H.; Nakayama, M.; Shintani, M.; Yamaoka, T.; Hayashi, H. *Bioorg. Med. Chem.* **2004**, *12*, 281–293.
- Yoshimura, K.; Kato, R.; Yusa, K.; Kavlick, M. F.; Maroun, V.; Nguyen, A.; Mimoto, T.; Ueno, T.; Shintani, M.; Falloon, J.; Masur, H.; Hayashi, H.; Erickson, J.; Mitsuya, H. *Proc. Natl. Acad. Sci. U.S.A.* **1999**, *96*, 8675–8680.
- Ghosh, A. K.; Thompson, W. J.; Holloway, M. K.; McKee, S. P.; Duong, T. T.; Lee, H. Y.; Munson, P. M.; Smith, A. M.; Wai, J. M.; Darke, P. L.; Zugay, J.; Emini, E. A.; Schleif, W. A.; Huff, J. R.; Anderson, P. S. *J. Med. Chem.* **1993**, *36*, 2300–2310.
- Ohmoto, K.; Okuma, M.; Yamamoto, T.; Kijima, H.; Sekioka, T.; Kitagawa, K.; Yamamoto, S.; Tanaka, K.; Kawabata, K.; Sakata, A., et al. *Bioorg. Med. Chem. Lett.* **2001**, *9*, 1307–1323.
- Ikunaka, M.; Matsumoto, J.; Nishimoto, Y. *Tetrahedron: Asymmetry* **2002**, *13*, 1201–1208.
- Iwona Kudyba, I.; Raczkowski, J.; Jurczak, J. *J. Org. Chem.* **2004**, *69*, 2844–2850.
- Ghosh, A. K.; Duong, T. T.; McKee, S. P. *Tetrahedron Lett.* **1992**, *33*, 2781–2784.
- (a) Ghosh, A. K.; Leshchenko, S.; Noetzel, M. *J. Org. Chem.* **2004**, *69*, 7822–7829; (b) Ghosh, A. K.; Gemma, S.; Takayama, J.; Baldrige, A.; Leshchenko-Yashchuk, S.; Miller, H. B.; Wang, Y.-F.; Kovalevsky, A. Y.; Koh, Y.; Weber, I. T.; Mitsuya, H. *Org. Biomol. Chem.* **2008**, *6*, 3703–3713; (c) Ghosh, A. K.; Gemma, S.; Baldrige, A.; Wang, Y.-F.; Kovalevsky, A. Y.; Koh, Y.; Weber, I. T.; Mitsuya, H. *J. Med. Chem.* **2008**, *51*, 6021–6033.
- Toth, M. V.; Marshall, G. R. A. *Int. J. Pep. Protein Res.* **1990**, *36*, 544–550.
- Vega, S.; Kang, L.-W.; Velazquez-Campoy, A.; Kiso, Y.; Amzel, L. M.; Freire, E. *Proteins* **2004**, *55*, 594–602.
- Kovalevski, A. Y.; Louis, J. M.; Aniana, A.; Ghosh, A. K.; Weber, I. T. *J. Mol. Biol.* **2008**, *384*, 178–192.



Neutralizing antibodies in SIV control: Co-impact with T cells

Hiroyuki Yamamoto, Tetsuro Matano*

International Research Center for Infectious Diseases, The Institute of Medical Science, The University of Tokyo, 4-6-1 Shirokanedai, Minato-ku, Tokyo 108-8639, Japan

ARTICLE INFO

Article history:

Received 15 May 2009

Received in revised form 19 August 2009

Accepted 18 September 2009

Keywords:

AIDS vaccine

Neutralizing antibody

Polyfunctional T-cell response

HIV-1

SIV

ABSTRACT

Human immunodeficiency virus type 1 (HIV-1) and pathogenic simian immunodeficiency virus (SIV)-infected naïve hosts experience a characteristic absence of early and potent virus-specific neutralizing antibody (NAb) responses preceding establishment of persistent infection. Yet conversely, we have recently shown that NABs passively immunized in rhesus macaques at early post-SIV challenge are capable of playing a critical role in non-sterile viremia control with implications of antibody-enhanced antigen presentation. In a current follow-up study we have further reported that NABs mediate rapid elicitation of polyfunctional virus-specific CD4⁺ T-cells *in vivo*. The NAB-immunized macaques mounting these responses exhibited sustained viremia control for over 1 year, accompanied with robust anti-SIV cellular immunity. Perspectives obtained from the results are discussed.

© 2009 Elsevier Ltd. All rights reserved.

1. Introduction: NAb absence in HIV-1/SIV acute infection

Absence of potent neutralizing antibody (NAb) responses in the very acute phase of human immunodeficiency virus type 1 (HIV-1) and simian immunodeficiency virus (SIV) infections is one major manifestation of defective adaptive immune responses in naïve hosts, generally failing in containment of virus replication unless privileged with certain genetic polymorphisms. HIV-1-specific NAB responses are unusually delayed in orders of months and hardly detected near peak infection. The primary humoral immune responses against these viruses are instead dominated by non-neutralizing virus-specific IgMs and IgGs [1] along with signs of aberrant polyclonal B-cell activation [2]. This initial failure is followed by a discordant array of NABs appearing in the subacute to chronic phase, each reaching considerable titers yet being permissive of continuous neutralization escape by the autologous virus [3–6]. A preferential and possibly consequent exhaustion of HIV-1-specific B-cell responses has also been indicated in the chronic phase [7]. With these backgrounds a prophylactic induction of NABs, particularly via pursuit of an optimal immunogen design eliciting a broadly neutralizing spectrum, has been a major aim in AIDS vaccine development [8].

Along with molecular analyses of NABs and the HIV-1/SIV envelope proteins known for their skewed antigenicity, protective activities of monoclonal and polyclonal NABs *in vivo* have been

assessed by passive immunization mainly in nonhuman primates. To date, vaccine regimens inducing satisfactory NAB titers even against homologous challenge strains have not yet been developed. Passive immunization currently is a first choice surrogate for NAB analysis, but they do hold certain advantageous aspects, such as being suited for examining their impact within a certain time zone of interest. Initial studies showed that NABs reaching a sufficient pre-challenge (or very early post-challenge) plasma or mucosal neutralizing titer typically render complete protection from chimeric simian/human immunodeficiency virus (SHIV) challenged via the same route [9–12], whereas titers to be attained for the viral inoculum sterilization had been a demanding one. On the other hand, it had been rather difficult to reach a consensus in determining whether NABs can exhibit anti-HIV-1/SIV activity in established infections. This was partly because the rapid memory CD4⁺ T-cell destructive nature of CCR5-tropic HIV-1 and pathogenic SIV had been clarified only recently [13,14], which turned out to differentially validate the moments of NAB infusion in each study retrospectively. For example, NABs passively administered in the chronic phase of HIV-1/SIV infection did not exert any impact on disease course even as a sequel to antiretroviral therapy in humans [15–16], while anti-SIV IG infusion at day 1 and day 14 post-SIVsmE660 challenge provided divergent viremia outcomes in infected macaques [17]. In HIV-1-inoculated human peripheral blood leukocyte-reconstituted SCID mice (hu-PBL-SCID mice), no suppressive effect was observed by NAB cocktail infusion past day 6 infection [18]. A common niche of these studies did however exist, which was the evaluation of the direct impact of NABs on pre-peak viral replication and what we had designed to assess in our system.

* Corresponding author. Tel.: +81 3 6409 2078; fax: +81 3 6409 2076.
E-mail address: matano@ims.u-tokyo.ac.jp (T. Matano).

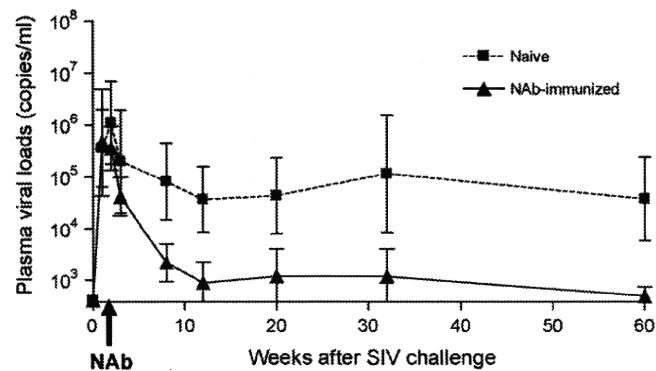


Fig. 1. Plasma viral loads in naïve controls and NAb-immunized macaques. Changes in geometric mean plasma viral loads in naïve controls (squares with dotted lines) and NAb-immunized macaques (triangles with bold lines) are shown. Error bars show the 95% confidence interval at each time point. The geometric mean plasma viral loads between weeks 12 and 60 were 5×10^4 copies/ml in naïve controls and $\leq 1 \times 10^3$ copies/ml NAb-immunized macaques.

2. Non-sterile SIV control via NABs

As an answer to this delineated question, we recently provided evidence for the clear potency of NABs to control established immunodeficiency virus replication in vivo by performing a post-infection NAB passive immunization in SIVmac239-challenged rhesus macaques [19]. While most SIVmac239-infected naïve macaques usually fail to elicit NAB responses during the early phase of infection, some acquire detectable levels of NABs against the challenge strain in the late phase. IgG purified from plasma of such SIVmac239-infected macaques with NAB induction, showing in vitro SIVmac239-specific neutralizing activity, was used for passive immunization as polyclonal anti-SIV NABs. These NABs were administered intravenously at day 7 post-SIVmac239 challenge, just before peak replication. The NAB passive immunization resulted in significant reduction of set-point viral loads (Fig. 1); this suppressive effect on viral replication became apparent (after week 5) past the limited duration (<1 week) of detectable NAB titers (Fig. 2). A notable observation in the NAB-immunized macaques was an accumulation of viral RNA in peripheral lymph node dendritic cells (DCs) within 24 h after the NAB infusion. Pulsing of DCs with NAB-bound SIV activated virus-specific CD4+ T cells in vitro with Fc-dependence, pointing out to a possibility of antibody-mediated virion uptake to DCs and facilitation of T-cell priming. This study thus unraveled that the existence of sub-sterile NABs near peak infection can indeed render significant suppressive activity against establishment of immunodeficiency virus persistent infection.

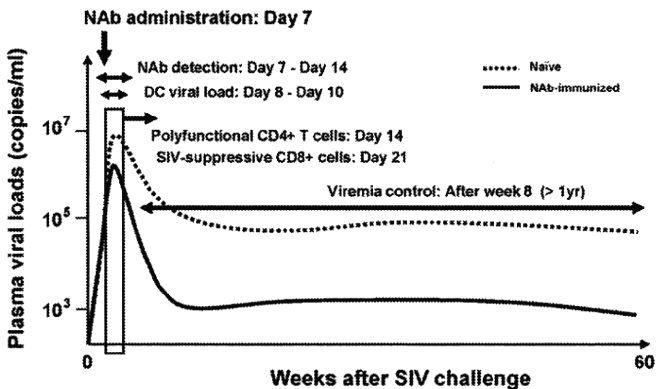


Fig. 2. Time-course events in NAB-mediated SIV control. The limited detection of plasma NAB titers between days 7 and 14 are concurrent with the rise in DC-viral loads (days 8–10), which is followed by appearance of Gag-specific CD4+ T cells with higher polyfunctionality at day 14 and CD8+ cells possessing higher anti-SIV efficacy at day 21 post-challenge. Plasma viral loads in the two groups start to show significant differences at week 8, and this is withheld up to week 60 post-challenge shown in Fig. 1. The box shows the critical time zone (weeks 1–2 post-challenge) to prime SIV-specific cellular immunity via NAB coexistence. Viral loads up to week 2 are drawn in a wider scale to ease visualization.

In our second follow-up study [20], the functional phenotypes of virus-specific T-cell responses in NAB-immunized macaques and naïve controls were further evaluated. Peripheral blood mononuclear cells (PBMCs) from both groups were pulsed with recombinant SIV Gag proteins in vitro, and SIV Gag-specific CD4+ T cells were assessed of their polyfunctionality via measurement of antigen-specific interferon- γ (IFN- γ), tumor necrosis factor- α (TNF- α), interleukin-2 (IL-2), macrophage inflammatory protein-1 β (MIP-1 β), and CD107a expression. The frequencies of polyfunctional Gag-specific CD4+ T cells, defined here as the upregulation of ≥ 3 of these five markers, were significantly elevated in the NAB-immunized macaques at day 14 post-challenge compared with naïve controls. Frequencies of these polyfunctional Gag-specific CD4+ T cells showed an inverse correlation with plasma viral loads at week 5, implying that early induction of these effectors was involved in the subsequent reduction of viremia.

In the chronic phase of infection (around week 30), Gag-specific CD4+ T-cell responses were detected in the NAB-immunized animals with higher polyfunctionality. These cells also showed their enhanced proliferative capacity as determined by SIV Gag-specific BrdU uptake. Accompanying these Gag-specific CD4+ T-cell responses, viral replication in the chronic phase remained significantly contained in the NAB-immunized macaques (Table 1 and Fig. 1). Three out of five animals exhibited undetectable plasma

Table 1
Summary of the passive NAB immunization experiment.

Animal	MHC-I haplotype	Ab-Tx at week 1 post-challenge ^a	Set-point VL (copies/ml)
Naïve controls			
R01-011	90-010-Ie	–	2×10^4 to 2×10^5
R01-012	90-010-Id	–	2×10^4 to 2×10^5
R03-005	90-030-Ig	–	1×10^3 to 2×10^4
R02-004	90-088-Ij	–	5×10^4 to 5×10^5
R02-021	ND ^b	Control Ab	3×10^5 to 6×10^6
R06-038	90-010-Ie	Control Ab	1×10^4 to 2×10^5
NAB-immunized			
R03-011	90-010-Ie	Anti-SIV NAB	$<4 \times 10^2$
R06-023	90-010-Id	Anti-SIV NAB	$<4 \times 10^2$
R03-020	ND	Anti-SIV NAB	1×10^3 to 2×10^4
R02-020	ND	Anti-SIV NAB	1×10^3 to 2×10^4
R03-013	90-030-Ih	Anti-SIV NAB	$<2 \times 10^3$

^a Macaques received no immunization (–) or passive immunization with control Abs or anti-SIVmac239 NABs intravenously at week 1 post-SIVmac239 challenge.
^b Not determined.

viral loads up to 60 weeks post-challenge, while the other two also maintained them at low levels lacking any palpable sign of control failure. De novo NABs were not detected in the NAB-immunized group, together suggesting that a single administration of NABs in acute SIV infection can result in long-term viremia control with appearance of robust virus-specific CD4+ T-cell responses.

Gag-specific CD8+ T-cell frequencies at day 14 post-challenge were simultaneously assessed in both groups, which revealed no significant differences in polyfunctionality between the two. The caveat here may have been the stimulation protocol, relying on cross-presentation of the pulsed recombinant SIV Gag protein which left room for a possibility of suboptimal virus-specific CTL examination. Therefore we alternatively attempted to assess their direct anti-SIV efficacy by performing an in vitro viral suppression assay (VSA). In this assay, CD8+ effector cells positively selected from PBMCs at week 3 post-infection were cocultured with autologous CD8-negative target cells pre-infected with SIV and peak virus production in the culture supernatant was measured [20]. CD8+ cells from three out of four examined NAB-immunized macaques showed nearly complete suppression of progeny virus production, a phenomenon not observed in any of the examined naïve controls. Notably, none of the NAB-immunized macaques possessed an MHC class I (MHC-I) haplotype 90-120-1a which has been previously shown to mount potent anti-SIV CTL responses. These data suggest that the NAB administration may help de novo induction of CD8+ cells exerting enhanced anti-SIV efficacy in vivo.

3. Significance of T-cell induction in NAB-mediated SIV control

Collectively these findings have depicted a previously undocumented pattern of immunodeficiency virus control, in that the early existence of NABs preceding peak SIV replication was followed by de novo appearance of polyfunctional Gag-specific CD4+ T cells (at week 2) and subsequent robust viremia control (after week 5) (Fig. 2). While the direct virus-neutralizing activity of the antibodies, as well as other effector functions such as antibody-dependent cell-mediated virus inhibition (ADCVI) [21,22] and/or complement activation [23] may have additively provided the protection of induced virus-specific CD4+ T cells from events such as DC trans-infection [24], the above sequence also coheres with our proposed possibility of NAB-mediated antigen presentation [19,25]. Antibody binding to soluble antigens is known to facilitate Fc-mediated uptake and resultant MHC class II antigen presentation in DCs [26,27], which renders the appearance of virus-specific polyfunctional CD4+ T cells in NAB-immunized macaques likely being a result of direct induction via NAB-mediated virion uptake into DCs.

An enigmatic role for HIV-1/SIV-specific CD4+ T cells has overall been posed in this regard of their potential vulnerability. While having been found of their presence as an inverse correlate of chronic phase viremia in HIV-1-infected humans [28], memory CD4+ T-cell subsets themselves (which likely include the virus-specific effectors) have been later determined as the primary target of CCR5-tropic primary AIDS-virus infections [15,29–32]. Detectable HIV-1-specific effector CD4+ T-cell responses in humans show an agreeable decline as viremia progresses [33], which may be driven by selective infection to some extent [34]. These are also in agreement with one study which documents prophylactic induction of Env-specific CD4+ T cells exerting a detrimental influence on the otherwise self-remitting course of SIVsmE660 viremia within that system [35]. In CTL-based prophylactic vaccines, acute and long-term preservation of (total and central) memory CD4+ T-cell counts has accordingly been defined as a passive correlate of protection status [36–38]. Hence the entity of truly contributable

HIV-1/SIV-specific CD4+ T-cell responses has overall not been clarified, although implications of their enrollment exist such as in relatively benign HIV-2 infection [39]. The current study newly supports two possibilities. One is that de novo polyfunctional Gag-specific effector CD4+ T cells, if induced, may be potent of actively driving primary viremia control; in other words, their existence can be taken as a cause rather than a result of protection. The other is that the antigen-specific activation potential of central memory CD4+ T cells is reinforced as a detailed protective correlate during chronic infection as in humans [28], in addition to the quantitative preservation of the subset. These two hallmarks in NAB-mediated SIV control sharply contrast Gag-specific CD4+ T-cell responses in naïve controls which, importantly, exhibit neither of the two.

It is important to question how these Gag-specific polyfunctional CD4+ T cells had exerted anti-SIV activity. Possibilities include roles such as conventional helper cells providing cognate assistance in priming CTLs for viremia clearance [40], effectors directly suppressing infected cells with [41,42] or without cytolytic activity, or both. Results of the CD8+ cell VSA in NAB-immunized macaques do not contradict participation of SIV-specific CTLs in acute phase viremia control, partially supporting the first candidate. When we performed VSA with CD8+ cells from the chronic phase (around week 20 post-challenge) in NAB-immunized macaques, no comparable in vitro virus suppression had been observed (unpublished results). This may also concur with the contracting levels of SIV-specific CTLs at low viral replication levels in vivo. Augmented virus-specific CTLs being a major, though maybe not the only, determinant of viremia suppression in the acute phase may be a reasonable explanation; if so, how their commitment may differ from viremia control in vaccinated and naïve SIV elite controllers (ECs) [43,44], or HIV-1 ECs in humans [45], is still unknown. Another factor to consider may be the Gag-specificity of these CD4+ T cells. As in CTLs, where importance of their Gag-biased induction in HIV-1/SIV viremia control has been emphasized both in vitro and in vivo [46,47], inducing CD4+ T-cell responses with a preference for Gag epitopes may also be advantageous in HIV-1/SIV control.

Regardless of the precise mechanism, there certainly lies a limitation to directly extrapolating results of this post-infection NAB passive immunization study to the patterns of protection likely afforded by endogenous NAB-inducing regimens. Nevertheless it is still important to recognize that the concordance of primary SIV control with de novo induction of polyfunctional Gag-specific CD4+ T cells, near the normal peak of systemic memory CD4+ T-cell destruction [14], does strengthen the rationale for prophylactic NAB induction. Even if induced NABs do not prevent the initial establishment of HIV-1/SIV infection, they may well exhibit their potential against systemic infection by a non-sterile protective mechanism. This narrow 1-week window around peak plasma viremia (Box in Fig. 2) is indeed some watershed for the HIV-1/SIV-infected host to impact viremia thereafter.

4. Perspectives: humoral and cellular immune concert for HIV-1 control

Whether or how cellular and humoral immune responses may collectively exert their effect against CCR5-tropic HIV-1/SIV acute infections had been unexplored, while systems involving other retroviruses have given some implications for this question. In Friend murine leukemia virus infection, high doses of administered pre-exposure NABs have provided an augmentation to memory T-cell-based control [48]. A similar augmentation does not, however, appear to happen in CXCR4-tropic SHIV89.6P infection [49]. Turning to a self-remitting benign SHIV infection (SHIV DH12R clone 8), the negative effect of CD20-depletion had only become apparent in macaques lacking a highly protective MHC-I allele

(Mamu-A*01), suggesting a seemingly interdependent rather than synergistic cooperation [50].

It is noteworthy that CD20+ B-cell depletion in the SIV/SHIV-macaque model is an interesting but intrinsically sensitive approach. What is problematic is that the outcome is complicated in a virus strain-dependent manner. In a pathogenic virus challenge (e.g., SIVmac) model the set-point viremia is significantly high. This seemingly blunts the effect of transient B-cell depletion from an incompetent baseline [51], while an impact on disease course appears to be partially observed in the subacute phase by constitutive B-cell depletion [52]. On the contrary, in models where relatively benign SIV (or SHIV) strains are challenged, host CTL responses reaching a certain threshold of potency may readily control viremia by themselves. The need of humoral immunity assistance is sufficiently compensated here, which again dampens the impact of B-cell depletion [53]. The propensity in such models seems to be that B-cell depletion effects only become appreciable in non-elite cellular immunity-eliciting controllers [50,54]. Since no detectable NABs are elicited in acute to subacute SIV infection, it likely follows that the cases of accelerated pathology via B-cell depletion may derive from the deprival of non-NAB-mediated effects, such as ADCVI. Taken together, the endogenous existence of antiviral non-neutralizing antibodies may change the outcome from rapid progression to persistent infection, whereas the exogenous administration of NABs may change the outcome from persistent infection to relative viremia control.

The entity of humoral immunity modulation against cellular immunity in HIV-1/SIV infection is hence still unclear; nevertheless one thing is becoming evident which is that, at least, NABs and T cells do not diminish each other in mere competitive coexistence for target elimination. Especially near peak SIV replication, NAB-dependent modification of T-cell immunity does exert a significant impact on viremia control.

In conclusion, there appears to be a preference of a balance, perhaps a temporal one, between induction of HIV-1/SIV-specific CD8+, CD4+ T cells and NABs. Determining the requisites for NAB-triggered T-cell immunity-based SIV replication control shall further reveal rational endpoints for prophylactic HIV-1 vaccines.

Conflict of interest statement

The authors state that they have no conflict of interest.

References

- [1] Tomaras GD, Yates NL, Liu P, Qin L, Fouda GG, Chavez LL, et al. Initial B-cell responses to transmitted human immunodeficiency virus type 1: virion-binding immunoglobulin M (IgM) and IgG antibodies followed by plasma anti-gp41 antibodies with ineffective control of initial viremia. *J Virol* 2008;82(24):12449–63.
- [2] De Milito A, Nilsson A, Titanji K, Thorstensson R, Reizenstein E, Narita M, et al. Mechanisms of hypergammaglobulinemia and impaired antigen-specific humoral immunity in HIV-1 infection. *Blood* 2004;103(6):2180–6.
- [3] Kwong PD, Doyle ML, Casper DJ, Cicala C, Leavitt SA, Majeed S, et al. HIV-1 evades antibody-mediated neutralization through conformational masking of receptor-binding sites. *Nature* 2002;420(6916):678–82.
- [4] Richman DD, Wrin T, Little SJ, Petropoulos CJ. Rapid evolution of the neutralizing antibody response to HIV type 1 infection. *Proc Natl Acad Sci USA* 2003;100(7):4144–9.
- [5] Wei X, Decker JM, Wang S, Hui H, Kappes JC, Wu X, et al. Antibody neutralization and escape by HIV-1. *Nature* 2003;422(6929):307–12.
- [6] Gray ES, Moore PL, Choge IA, Decker JM, Bibollet-Ruche F, Li H, et al. Neutralizing antibody responses in acute human immunodeficiency virus type 1 subtype C infection. *J Virol* 2007;81(12):6187–96.
- [7] Moir S, Ho J, Malaspina A, Wang W, DiPoto AC, O'Shea MA, et al. Evidence for HIV-associated B cell exhaustion in a dysfunctional memory B cell compartment in HIV-infected viremic individuals. *J Exp Med* 2008;205(8):1797–805.
- [8] Burton DR, Desrosiers RC, Doms RW, Koff WC, Kwong PD, Moore JP, et al. HIV vaccine design and the neutralizing antibody problem. *Nat Immunol* 2004;5(3):233–6.
- [9] Shibata R, Igarashi T, Haigwood N, Buckler-White A, Ogert R, Ross W, et al. Neutralizing antibody directed against the HIV-1 envelope glycoprotein can completely block HIV-1/SIV chimeric virus infections of macaque monkeys. *Nat Med* 1999;5(2):204–10.
- [10] Mascola JR, Lewis MG, Stiegler G, Harris D, VanCott TC, Hayes D, et al. Protection of Macaques against pathogenic simian/human immunodeficiency virus 89.6PD by passive transfer of neutralizing antibodies. *J Virol* 1999;73(5):4009–18.
- [11] Mascola JR, Stiegler G, VanCott TC, Katinger H, Carpenter CB, Hanson CE, et al. Protection of macaques against vaginal transmission of a pathogenic HIV-1/SIV chimeric virus by passive infusion of neutralizing antibodies. *Nat Med* 2000;6(2):207–10.
- [12] Nishimura Y, Igarashi T, Haigwood NL, Sadjadpour R, Donau OK, Buckler C, et al. Transfer of neutralizing IgG to macaques 6 h but not 24 h after SHIV infection confers sterilizing protection: implications for HIV-1 vaccine development. *Proc Natl Acad Sci USA* 2003;100(25):15131–6.
- [13] Nishimura Y, Igarashi T, Donau OK, Buckler-White A, Buckler C, Lafont BA, et al. Highly pathogenic SHIVs and SIVs target different CD4+ T cell subsets in rhesus monkeys, explaining their divergent clinical courses. *Proc Natl Acad Sci USA* 2004;101(33):12324–9.
- [14] Mattapallil JJ, Douek DC, Hill B, Nishimura Y, Martin M, Roederer M. Massive infection and loss of memory CD4+ T cells in multiple tissues during acute SIV infection. *Nature* 2005;434(7037):1093–7.
- [15] Trkola A, Kuster H, Rusert P, Joos B, Fischer M, Leemann C, et al. Delay of HIV-1 rebound after cessation of antiretroviral therapy through passive transfer of human neutralizing antibodies. *Nat Med* 2005;11(6):615–22.
- [16] Binley JM, Clas B, Gettie A, Vesanen M, Montefiori DC, Sawyer L, et al. Passive infusion of immune serum into simian immunodeficiency virus-infected rhesus macaques undergoing a rapid disease course has minimal effect on plasma viremia. *Virology* 2000;270(1):237–49.
- [17] Haigwood NL, Watson A, Sutton WF, McClure J, Lewis A, Ranchalis J, et al. Passive immune globulin therapy in the SIV/macaque model: early intervention can alter disease profile. *Immunol Lett* 1996;51(1–2):107–14.
- [18] Pognard P, Sabbe R, Picchio GR, Wang M, Culizia RJ, Katinger H, et al. Neutralizing antibodies have limited effects on the control of established HIV-1 infection in vivo. *Immunity* 1999;10(4):431–8.
- [19] Yamamoto H, Kawada M, Takeda A, Igarashi H, Matano T. Post-infection immunodeficiency virus control by neutralizing antibodies. *PLoS ONE* 2007;2(6):e540.
- [20] Yamamoto T, Iwamoto N, Yamamoto H, Tsukamoto T, Kuwano T, Takeda A, et al. Polyfunctional CD4+ T-Cell induction in neutralizing antibody-triggered control of simian immunodeficiency virus infection. *J Virol* 2009;83(11):5514–24.
- [21] Forthal DN, Landucci G, Daar ES. Antibody from patients with acute human immunodeficiency virus (HIV) infection inhibits primary strains of HIV type 1 in the presence of natural-killer effector cells. *J Virol* 2001;75(15):6953–61.
- [22] Hessel AJ, Hangartner L, Hunter M, Havenith CE, Beurskens FJ, Bakker JM, et al. Fc receptor but not complement binding is important in antibody protection against HIV. *Nature* 2007;449(7158):101–4.
- [23] Huber M, Fischer M, Misselwitz B, Manrique A, Kuster H, Niederöst B, et al. Complement lysis activity in autologous plasma is associated with lower viral loads during the acute phase of HIV-1 infection. *PLoS Med* 2006;3(11):e441.
- [24] Frankel SS, Steinman RM, Michael NL, Kim SR, Bhardwaj N, Pope M, et al. Neutralizing monoclonal antibodies block human immunodeficiency virus type 1 infection of dendritic cells and transmission to T cells. *J Virol* 1998;72(12):9788–94.
- [25] Yamamoto H, Matano T. Anti-HIV adaptive immunity: determinants for viral persistence. *Rev Med Virol* 2008;18(5):293–303.
- [26] Sallusto F, Lanzavecchia A. Efficient presentation of soluble antigen by cultured human dendritic cells is maintained by granulocyte/macrophage colony-stimulating factor plus interleukin 4 and downregulated by tumor necrosis factor alpha. *J Exp Med* 1994;179(4):1109–18.
- [27] Cella M, Engering A, Pinet V, Peters J, Lanzavecchia A. Inflammatory stimuli induce accumulation of MHC class II complexes on dendritic cells. *Nature* 1997;388(6644):782–7.
- [28] Rosenberg ES, Billingsley JM, Caliendo AM, Boswell SL, Sax PE, Kalams SA, et al. Vigorous HIV-1-specific CD4+ T cell responses associated with control of viremia. *Science* 1997;278(5342):1447–50.
- [29] Veazey RS, DeMaria M, Chalifoux LV, Shvetz DE, Pauley DR, Knight HL, et al. Gastrointestinal tract as a major site of CD4+ T cell depletion and viral replication in SIV infection. *Science* 1998;280(5362):427–31.
- [30] Brenchley JM, Schacker TW, Ruff LE, Price DA, Taylor JH, Beilman GJ, et al. CD4+ T cell depletion during all stages of HIV disease occurs predominantly in the gastrointestinal tract. *J Exp Med* 2004;200(6):749–59.
- [31] Picker LJ, Hagen SI, Lum R, Reed-Inderbitzin EF, Daly LM, Sylwester AW, et al. Insufficient production and tissue delivery of CD4+ memory T cells in rapidly progressive simian immunodeficiency virus infection. *J Exp Med* 2004;200(10):1299–314.
- [32] Li Q, Duan L, Estes JD, Ma ZM, Rourke T, Wang Y, et al. Peak SIV replication in resting memory CD4+ T cells depletes gut lamina propria CD4+ T cells. *Nature* 2005;434(7037):1148–52.
- [33] Zaunders JJ, Munier ML, Kaufmann DE, Ip S, Grey P, Smith D, et al. Early proliferation of CCR5(+) CD38(+++) antigen-specific CD4(+) Th1 effector cells during primary HIV-1 infection. *Blood* 2005;106(5):1660–7.

- [34] Douek DC, Brenchley JM, Betts MR, Ambrozak DR, Hill BJ, Okamoto Y, et al. HIV preferentially infects HIV-specific CD4⁺ T cells. *Nature* 2002;417(6884):95–8.
- [35] Staprans SI, Barry AP, Silvestri G, Safrit JT, Kozyr N, Sumpter B, et al. Enhanced SIV replication and accelerated progression to AIDS in macaques primed to mount a CD4 T cell response to the SIV envelope protein. *Proc Natl Acad Sci USA* 2004;101(35):13026–31.
- [36] Letvin NL, Mascola JR, Sun Y, Gorgone DA, Buzby AP, Xu L, et al. Preserved CD4⁺ central memory T cells and survival in vaccinated SIV-challenged monkeys. *Science* 2006;312(5779):1530–3.
- [37] Mattapallil JJ, Douek DC, Buckler-White A, Montefiori D, Letvin NL, Nabel GJ, et al. Vaccination preserves CD4 memory T cells during acute simian immunodeficiency virus challenge. *J Exp Med* 2006;203(6):1533–41.
- [38] Wilson NA, Reed J, Napoe GS, Piaskowski S, Szymanski A, Furlott J, et al. Vaccine-induced cellular immune responses reduce plasma viral concentrations after repeated low-dose challenge with pathogenic simian immunodeficiency virus SIVmac239. *J Virol* 2006;80(12):5875–85.
- [39] Duvall MG, Jaye A, Dong T, Brenchley JM, Alabi AS, Jeffries DJ, et al. Maintenance of HIV-specific CD4⁺ T cell help distinguishes HIV-2 from HIV-1 infection. *J Immunol* 2006;176(11):6973–81.
- [40] Castellino F, Germain RN. Cooperation between CD4⁺ and CD8⁺ T cells: when, where, and how. *Annu Rev Immunol* 2006;24:519–40.
- [41] Gauduin MC, Yu Y, Barabasz A, Carville A, Piatak M, Lifson JD, et al. Induction of a virus-specific effector-memory CD4⁺ T cell response by attenuated SIV infection. *J Exp Med* 2006;203(12):2661–72.
- [42] Casazza JP, Betts MR, Price DA, Precopio ML, Ruff LE, Brenchley JM, et al. Acquisition of direct antiviral effector functions by CMV-specific CD4⁺ T lymphocytes with cellular maturation. *J Exp Med* 2006;203(13):2865–77.
- [43] Matano T, Kobayashi M, Igarashi H, Takeda A, Nakamura H, Kano M, et al. T lymphocyte-based control of simian immunodeficiency virus replication in a preclinical AIDS vaccine trial. *J Exp Med* 2004;199(12):1709–18.
- [44] Friedrich TC, Valentine LE, Yant LJ, Rakasz EG, Piaskowski SM, Furlott JR, et al. Subdominant CD8⁺ T-cell responses are involved in durable control of AIDS virus replication. *J Virol* 2007;81(7):3465–76.
- [45] Betts MR, Nason MC, West SM, De Rosa SC, Migueles SA, Abraham J, et al. HIV nonprogressors preferentially maintain highly functional HIV-specific CD8⁺ T cells. *Blood* 2006;107(12):4781–9.
- [46] Sacha JB, Chung C, Rakasz EG, Spencer SP, Jonas AK, Bean AT, et al. Gag-specific CD8⁺ T lymphocytes recognize infected cells before AIDS-virus integration and viral protein expression. *J Immunol* 2007;178(5):2746–54.
- [47] Kiepiela P, Ngumbela K, Thobakgale C, Ramduth D, Honeyborne I, Moodley E, et al. CD8⁺ T-cell responses to different HIV proteins have discordant associations with viral load. *Nat Med* 2007;13(1):46–53.
- [48] Messer RJ, Dittmer U, Peterson KE, Hasenkrug KJ. Essential role for virus-neutralizing antibodies in sterilizing immunity against Friend retrovirus infection. *Proc Natl Acad Sci USA* 2004;101(33):12260–5.
- [49] Mascola JR, Lewis MG, VanCott TC, Stiegler G, Katinger H, Seaman M, et al. Cellular immunity elicited by human immunodeficiency virus type 1/simian immunodeficiency virus DNA vaccination does not augment the sterile protection afforded by passive infusion of neutralizing antibodies. *J Virol* 2003;77(19):10348–56.
- [50] Mao H, Lafont BA, Igarashi T, Nishimura Y, Brown C, Hirsch V, et al. CD8⁺ and CD20⁺ lymphocytes cooperate to control acute simian immunodeficiency virus/human immunodeficiency virus chimeric virus infections in rhesus monkeys: modulation by major histocompatibility complex genotype. *J Virol* 2005;79(23):14887–98.
- [51] Schmitz JE, Kuroda MJ, Santra S, Simon MA, Lifton MA, Lin W, et al. Effect of humoral immune responses on controlling viremia during primary infection of rhesus monkeys with simian immunodeficiency virus. *J Virol* 2003;77(3):2165–73.
- [52] Miller CJ, Genesca M, Abel K, Montefiori D, Forthal D, Bost K, et al. Antiviral antibodies are necessary for control of simian immunodeficiency virus replication. *J Virol* 2007;81(10):5024–35.
- [53] Gaufin T, Gautam R, Kasheta M, Ribeiro R, Ribka E, Barnes M, et al. Limited ability of humoral immune responses in control of viremia during infection with SIVsmmD215 strain. *Blood* 2009;113(18):4250–61.
- [54] Johnson WE, Lifson JD, Lang SM, Johnson RP, Desrosiers RC. Importance of B-cell responses for immunological control of variant strains of simian immunodeficiency virus. *J Virol* 2003;77(1):375–81.

Broadening of CD8⁺ cell responses in vaccine-based simian immunodeficiency virus controllers

Nami Iwamoto^a, Tetsuo Tsukamoto^a, Miki Kawada^a, Akiko Takeda^a,
Hiroyuki Yamamoto^a, Hiroaki Takeuchi^a and Tetsuro Matano^{a,b}

Objective: In our prior study on a prophylactic T-cell-based vaccine, some vaccinated macaques controlled a simian immunodeficiency virus (SIV) challenge. These animals allowed viremia in the acute phase but showed persistent viral control after the setpoint. Here, we examined the breadth of postchallenge virus-specific cellular immune responses in these SIV controllers.

Design: We previously reported that in a group of Burmese rhesus macaques possessing the MHC haplotype *90-120-Ia*, immunization with a Gag-expressing vaccine results in nonsterile control of a challenge with SIVmac239 but not a mutant SIV carrying multiple cytotoxic T lymphocyte (CTL) escape gag mutations. In the present study, we investigated whether broader cellular immune responses effective against the mutant SIV replication are induced after challenge in those vaccinees that maintained wild-type SIVmac239 control.

Methods: We analyzed cellular immune responses in these SIV controllers ($n = 8$).

Results: These controllers elicited CTL responses directed against SIV non-Gag antigens as well as Gag in the chronic phase. Postvaccinated, prechallenge CD8⁺ cells obtained from these animals suppressed wild-type SIV replication *in vitro*, but mostly had no suppressive effect on the mutant SIV replication, whereas CD8⁺ cells in the chronic phase after challenge showed efficient antimutant SIV efficacy. The levels of *in vitro* antimutant SIV efficacy of CD8⁺ cells correlated with Vif-specific CD8⁺ T-cell frequencies. Plasma viremia was kept undetectable even after the mutant SIV superchallenge in the chronic phase.

Conclusion: These results suggest that vaccine-based wild-type SIV controllers can acquire CD8⁺ cells with the potential to suppress replication of SIV variants carrying CTL escape mutations.

© 2010 Wolters Kluwer Health | Lippincott Williams & Wilkins

AIDS 2010, **24**:2777–2787

Keywords: AIDS vaccine, cytotoxic T lymphocyte, major histocompatibility complex, mutation, simian immunodeficiency virus

Introduction

Virus-specific CD8⁺ cytotoxic T lymphocyte (CTL) responses are crucial for the control of HIV and simian immunodeficiency virus (SIV) replication [1–6]. Cumulative studies on HIV-infected individuals have shown association of HLA genotypes with rapid or delayed AIDS progression [7,8]. For instance, most of the HIV-infected

individuals possessing *HLA-B*57* have been indicated to show a better prognosis with lower viral loads, implicating *HLA-B*57*-restricted epitope-specific CTL responses in this viral control [9–11]. Indian rhesus macaques possessing particular major histocompatibility complex class I (MHC-I) alleles such as Mamu-B*17 tend to show SIV control [12–14]. These imply possible HIV control by induction of particular effective CTL responses.

^aInternational Research Center for Infectious Diseases, The Institute of Medical Science, The University of Tokyo, and ^bAIDS Research Center, National Institute of Infectious Diseases, Tokyo, Japan.

Correspondence to Tetsuro Matano, International Research Center for Infectious Diseases, The Institute of Medical Science, The University of Tokyo, 4-6-1 Shirokanedai, Minato-ku, Tokyo 108-8639, Japan.

Tel: +81 3 6409 2078; fax: +81 3 6409 2076; e-mail: matano@ims.u-tokyo.ac.jp

Received: 19 June 2010; revised: 23 August 2010; accepted: 1 September 2010.

DOI:10.1097/QAD.0b013e3283402206

ISSN 0269-9370 © 2010 Wolters Kluwer Health | Lippincott Williams & Wilkins

Copyright © Lippincott Williams & Wilkins. Unauthorized reproduction of this article is prohibited.

2777

Recent trials of prophylactic T-cell-based vaccines in macaque AIDS models have indicated a possibility of reduction in postchallenge viral loads [15–20]. We previously developed a prophylactic AIDS vaccine consisting of a DNA prime followed by a boost with a Sendai virus (SeV) vector expressing SIVmac239 Gag (SeV-Gag) [21,22]. Our trial showed vaccine-based control of a SIVmac239 challenge in a group of Burmese rhesus macaques sharing the MHC-I haplotype 90–120-Ia; these 90–120-Ia-positive vaccinees dominantly elicited Gag_{206–216} (IINEEAADWDL) epitope-specific and Gag_{241–249} (SSVDEQIQW) epitope-specific CTL responses and contained SIVmac239 replication after challenge [15,23]. In contrast, 90–120-Ia-positive vaccinees failed to control a challenge with a mutant virus, SIVmac239Gag216S244E247L312V373T (referred to as SIV-G64723mt), which carries five gag mutations resulting in escape from recognition by Gag-specific CTLs including Gag_{206–216}-specific and Gag_{241–249}-specific CTLs. This indicates that these CTL responses play a crucial role in the vaccine-based primary control of wild-type SIVmac239 replication [24]. Furthermore, in a SIVmac239 challenge experiment of 90–120-Ia-positive rhesus macaques that received a prophylactic vaccine expressing the Gag_{241–249} epitope fused with enhanced green fluorescent protein (EGFP), this single epitope vaccination resulted in control of SIVmac239 replication with dominant induction of Gag_{241–249}-specific CTL responses in the acute phase after challenge [25]. We refer to these vaccinated animals that controlled viral replication after wild-type SIVmac239 challenge as SIV controllers in the present study.

Administration of SIV controllers with a monoclonal anti-CD8 antibody (i.e., CD8 depletion after the establishment of primary viral control) has suggested that CD8⁺ cell responses play an important role in maintaining the viral control in the chronic phase [26,27]. Then, it is of great concern whether these wild-type SIV controllers can acquire CD8⁺ cells effective against replication of SIV variants escaping from dominant CTL responses. In the present study, we have analyzed 90–120-Ia-positive vaccinees controlling a SIVmac239 challenge in order to examine whether 90–120-Ia-positive animals can elicit cellular immune responses effective against the mutant SIV, SIV-G64723mt, carrying multiple CTL escape gag mutations. Our analyses in these vaccine-based SIV controllers revealed dynamics of virus-specific cellular immune responses during persistent viral control and suggested postchallenge induction of CD8⁺ cells able to suppress replication of SIV variants carrying CTL escape mutations.

Materials and methods

SIV-G64723mt

The SIV-G64723mt (SIVmac239Gag216S244E247L312V373T) carries five gag mutations, GagL216S (leading

to a leucine [L]-to-serine [S] substitution at the 216th amino acid in Gag, GagD244E (aspartic acid [D]-to-glutamic acid [E] at the 244th amino acid), GagI247L (isoleucine [I] to L at the 247th amino acid), GagA312V (alanine [A] to valine [V] at the 312th amino acid), and GagA373T (A to threonine [T] at the 373rd amino acid), which were selected, at the cost of viral fitness, in a SIVmac239-infected macaque possessing the MHC-I haplotype 90–120-Ia, as described previously [23,28]. GagL216S, GagD244E, GagI247L, and GagA373T mutations, which became dominant mostly in SIVmac239-infected 90–120-Ia-positive rhesus macaques, result in viral escape from recognition by Gag_{206–216}-specific, Gag_{241–249}-specific, and Gag_{373–380}-specific CTLs, respectively, whereas it remains unclear whether GagA312V was selected for by CTLs.

Animal experiments

Eight Burmese rhesus macaques (*Macaca mulatta*) possessing the MHC-I haplotype 90–120-Ia, which showed vaccine-based control of a SIVmac239 challenge, were used in this study and divided into two groups (Fig. 1a). Five macaques, R06-015, R03-014, R03-012, R02-002, and R02-003, in group I received a prophylactic DNA prime/SeV-Gag boost vaccine (referred to as DNA/SeV-Gag vaccine) and contained SIVmac239 challenge as reported previously [15,24,29]. The DNA used for the vaccination, CMV-SHIVdEN [15], was constructed from *env*-deleted and *nef*-deleted simian–human immunodeficiency virus SHIV_{MD14YE} [30] molecular clone DNA (SIVGP1) and has the genes encoding SIVmac239 Gag, Pol, Vif, and Vpx, SIVmac239-HIV chimeric Vpr, and HIV Tat and Rev. At the DNA vaccination, animals received 5 mg of CMV-SHIVdEN DNA intramuscularly. Six weeks after the DNA prime, animals received a single boost intranasally with 6×10^9 cell infectious units (CIUs) of F-deleted replication-defective SeV-Gag [31,32]. At week 1 after SIV challenge, macaque R03-014 was inoculated with nonspecific immunoglobulin G (IgG), and macaques R03-012 and R02-002 with IgG purified from neutralizing antibody-positive plasma of chronically SIV-infected macaques in our previous study [29]. Two macaques R04-016 and R06-007 in group II received a prophylactic prime-boost vaccine eliciting single Gag_{241–249} epitope-specific CTL responses (referred to as DNA/SeV-Gag_{236–250}-EGFP vaccine) and contained SIVmac239 challenge as reported previously [25]. In this vaccine protocol, animals were primed with 5 mg of pGag_{236–250}-EGFP-N1 DNA expressing a Gag_{236–250}-EGFP fusion protein, followed by a boost with 6×10^9 CIU of F-deleted SeV expressing the Gag_{236–250}-EGFP fusion protein (SeV-Gag_{236–250}-EGFP). Macaque R04-015 in group II received a prophylactic prime-boost vaccine eliciting Gag_{206–216} epitope-specific and Gag_{241–249} epitope-specific CTL responses (referred to as DNA/SeV-Gag_{202–216}-EGFP and DNA/SeV-Gag_{236–250}-EGFP vaccine); this animal was primed with pGag_{202–216}-EGFP-N1 and pGag_{236–}

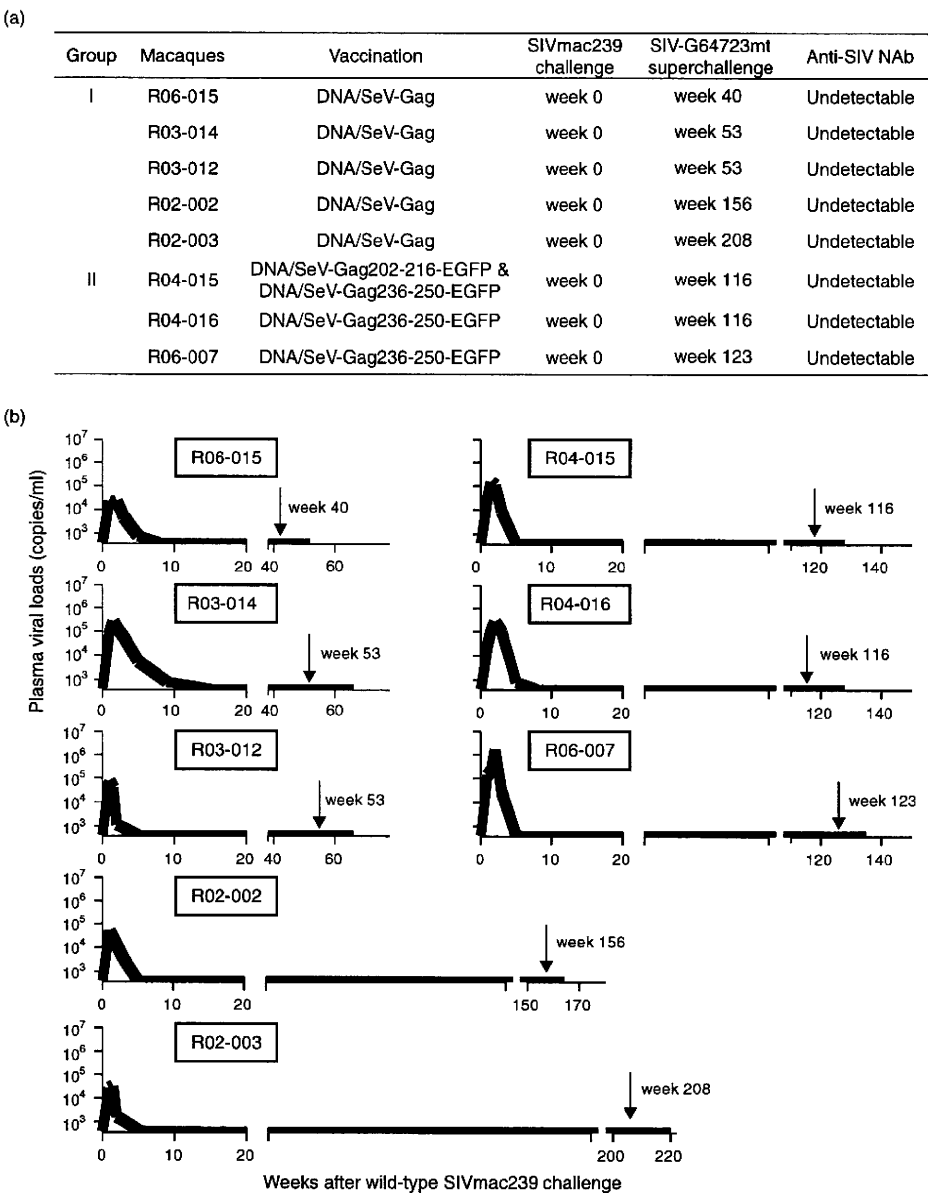


Fig. 1. Plasma viral loads in simian immunodeficiency virus controllers. (a) The list of rhesus macaques used in this study. All are *90-120-1a*-positive. SIVmac239-specific neutralizing antibody (anti-SIV NAb) responses just before the mutant SIV superchallenge were undetectable. (b) Plasma viral loads (SIV *gag* RNA copies/ml plasma) determined as described previously [15]. The lower limit of detection is approximately 4×10^2 copies/ml. The arrows indicate the time points of SIV-G64723mt superchallenge. SIV, simian immunodeficiency virus.

²⁵⁰-EGFP-N1 DNAs, followed by a boost with SeV-Gag₂₀₂₋₂₁₆-EGFP and SeV-Gag₂₃₆₋₂₅₀-EGFP. Both pGag₂₀₂₋₂₁₆-EGFP-N1 and SeV-Gag₂₀₂₋₂₁₆-EGFP express a Gag₂₀₂₋₂₁₆-EGFP fusion protein [33]. These vaccinated animals were challenged intravenously with 1000 50% tissue culture infective doses (TCID₅₀) of SIVmac239 [34] approximately 3 months after the boost and were superchallenged intravenously with 1000 TCID₅₀ of SIV-G64723mt in the chronic phase. The challenge virus stocks were prepared by virus propagation on rhesus macaque peripheral blood mononuclear cells

(PBMCs). All animals were maintained in accordance with the guidelines for animal experiments at the National Institute of Infectious Diseases.

In-vitro viral suppression assay

To evaluate in-vitro anti-SIVmac239 or anti-SIV-G64723mt efficacy of CD8⁺ cells, we examined SIVmac239 or SIV-G64723mt replication on CD8-depleted PBMCs in the presence of CD8⁺ cells positively selected from macaque PBMCs as described previously [27,35]. In brief, PBMCs were separated into CD8⁺ and

CD8⁺ cells by using Macs CD8 MicroBeads (Miltenyi Biotec, Tokyo, Japan). For preparing target cells, the CD8⁺ cells selected from PBMCs obtained before SIVmac239 challenge were cultured in the presence of 2 µg/ml phytohemagglutinin L and 20 IU/ml recombinant human interleukin-2 (Roche Diagnostics, Tokyo, Japan) and infected with SIVmac239 at a multiplicity of infection (MOI) of 1:10³ TCID₅₀/cell or with SIV-G64723mt at MOI of 1:10² TCID₅₀/cell, using the virus stocks prepared by virus propagation on HSC-F cells (herpesvirus saimiri-immortalized macaque T-cell line) [36]. SIV-G64723mt with lower replicative ability was added at higher MOI to show similar replication kinetics with SIVmac239 replication in the control culture without CD8⁺ cells. Target cells were cultured for 2 days and then effector CD8⁺ cells selected from PBMCs obtained 1 week after boost or at several time points after the challenge were added to the target cells at an effector : target (*E* : *T*) ratio of 1 : 4. Reverse transcriptase activities in these culture supernatants were measured [37] to determine the peak of viral production in the control culture of target cells without CD8⁺ cells. RNA was extracted from culture supernatants at the peak using the high pure viral RNA Kit (Roche Diagnostics) and viral RNA levels were measured by LightCycler system (Roche Diagnostics) using SIV *gag*-specific primers (GTAGTATGGGCAGCAATGA and TGTTCCTGTTTCCACCACTA) and probes (GCATTCACGCA GAAGAGAAAGTGAAACA-Flu and LCRed-ACTG AGGAAGCAAAACAGATAGTGCAGAGA) (Nihon Gene Research Laboratories Inc., Sendai, Japan). Reduction in viral production by addition of each group of CD8⁺ cells was shown as reduction (fold) in viral RNA level compared with that in the supernatant from virus-infected CD8⁺ cell culture without CD8⁺ cells.

Analysis of virus-specific CD8⁺ T-cell responses

We measured virus-specific CD8⁺ T-cell levels by flow cytometric analysis of gamma interferon (IFN-γ) induction after specific stimulation as described previously [15]. In brief, PBMCs were cocultured for 6 h with autologous herpesvirus papio-immortalized B-lymphoblastoid cell lines pulsed with 1 µmol/l SIVmac239 Gag₂₀₆₋₂₁₆, Gag₂₄₁₋₂₄₉, or Gag₃₆₇₋₃₈₁ peptides for Gag₂₀₆₋₂₁₆-specific, Gag₂₄₁₋₂₄₉-specific, or Gag₃₆₇₋₃₈₁-specific stimulation. Alternatively, PBMCs were cocultured with B-lymphoblastoid cell lines pulsed with peptide pools using panels of overlapping peptides spanning the entire SIVmac239 Gag, Pol, Vif, Vpx, Vpr, Tat, Rev, Nef, and Env amino acid sequences. Intracellular IFN-γ staining was performed using a Cytofix/Cytoperm kit (BD, Tokyo, Japan) and fluorescein isothiocyanate-conjugated antihuman CD4, peridinin chlorophyll protein-conjugated antihuman CD8, allophycocyanin-conjugated antihuman CD3, and phycoerythrin-conjugated antihuman IFN-γ monoclonal antibodies (BD). Specific CD8⁺ T-cell levels were calculated by subtracting nonspecific IFN-γ⁺ CD8⁺ T-cell fre-

quencies from those after peptide-specific stimulation. Specific CD8⁺ T-cell levels lower than 100 per million PBMCs were considered negative.

Analysis of virus-specific neutralizing antibody responses

SIVmac239-specific neutralizing antibody responses were examined by determining the end point plasma titers for inhibiting 10 TCID₅₀ virus replication as described previously [26]. Serial two-fold dilutions of heat-inactivated plasma were prepared in quadruplicate and mixed with 10 TCID₅₀ of SIVmac239. In each culture, 5 µl of virus was incubated with 5 µl of plasma for 45 min and was added to 5 × 10⁴ MT4 cells. Reverse transcriptase activities in the culture supernatants on day 12 were measured to determine the 100% neutralizing endpoint. The lower limit of detection is a titer of 1 : 2.

Statistical analysis

Statistical analysis was performed using Prism software version 4.03 (GraphPad Software Inc., San Diego, California, USA) with significance levels set at a *P* value of less than 0.05. Specific CD8⁺ T-cell frequencies and in-vitro anti-SIV efficacy levels (fold of reduction in viral production) were log transformed and correlation was analyzed by the Pearson test.

Results

Anti-SIVmac239 and anti-SIV-G64723mt efficacy *in vitro* of CD8⁺ cells in simian immunodeficiency virus controllers

We analyzed eight 90–120-Ia-positive rhesus macaques that showed vaccine-based control of a SIVmac239 challenge (Fig. 1a). These SIV controllers were divided into group I consisting of five animals (R06-015, R03-014, R03-012, R02-002, and R02-003) vaccinated with DNA/SeV-Gag [15] and group II consisting of one animal (R04-015) vaccinated with DNA/SeV-Gag₂₀₂₋₂₁₆-EGFP and DNA/SeV-Gag₂₃₆₋₂₅₀-EGFP and two (R04-016 and R06-007) vaccinated with DNA/SeV-Gag₂₃₆₋₂₅₀-EGFP [25]. After an intravenous challenge with SIVmac239, all of these macaques showed viremia in the acute phase, but then controlled viral replication; plasma viremia was undetectable after the setpoint (Fig. 1b).

First, we investigated the potential of macaque CD8⁺ cells obtained at several time points, after boost but before SIVmac239 challenge (referred to as postboost) and after challenge, to suppress SIVmac239 (Fig. 2) or SIV-G64723mt (Fig. 3) replication by in-vitro viral suppression assay [27,38–40]. In this assay, PBMC-derived CD8⁺ target cells infected with SIVmac239 or SIV-G64723mt were cocultured with effector CD8⁺ cells from PBMCs obtained at several time points at an *E*/*T*

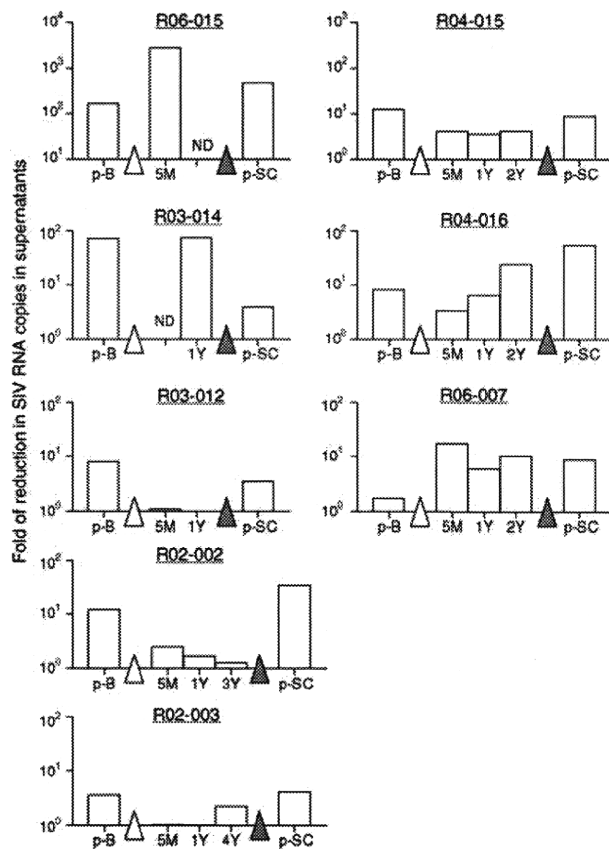


Fig. 2. Anti-SIVmac239 efficacy *in vitro* of CD8⁺ cells in simian immunodeficiency virus controllers. PBMC-derived CD8⁺ (target) cells infected with SIVmac239 were cultured alone or cocultured with autologous PBMC-derived CD8⁺ (effector) cells at several time points at an *E:T* ratio of 1:4. The ratios of viral RNA levels in the supernatants from the coculture to those without CD8⁺ cells are shown. ND: not determined. p-B: 1 week after boost; 5M, 1Y, 2Y, 3Y, and 4Y: 5 months, 1, 2, 3, and 4 years after challenge, respectively; p-SC: 1 or 2 months after superchallenge. Open triangles indicate the time points of SIVmac239 challenge and closed triangles SIV-G64723mt superchallenge. PBMC, peripheral blood mononuclear cell; SIV, simian immunodeficiency virus.

ratio of 1:4, and viral production in culture supernatants was examined to assess suppressive effect of CD8⁺ cells on viral replication *in vitro*.

CD8⁺ cells 1 week after boost mostly suppressed wild-type SIVmac239 replication efficiently. In contrast, these postboost CD8⁺ cells failed to show efficient suppressive effect on SIV-G64723mt replication. These results suggest that Gag₂₀₆₋₂₁₆-specific, Gag₂₄₁₋₂₄₉-specific, and Gag₃₆₇₋₃₈₁-specific CTL responses play a central role in the suppression of SIVmac239 replication by postboost CD8⁺ cells.

After SIVmac239 challenge, all these animals showed efficient *in-vitro* anti-SIV-G64723mt efficacy (more than

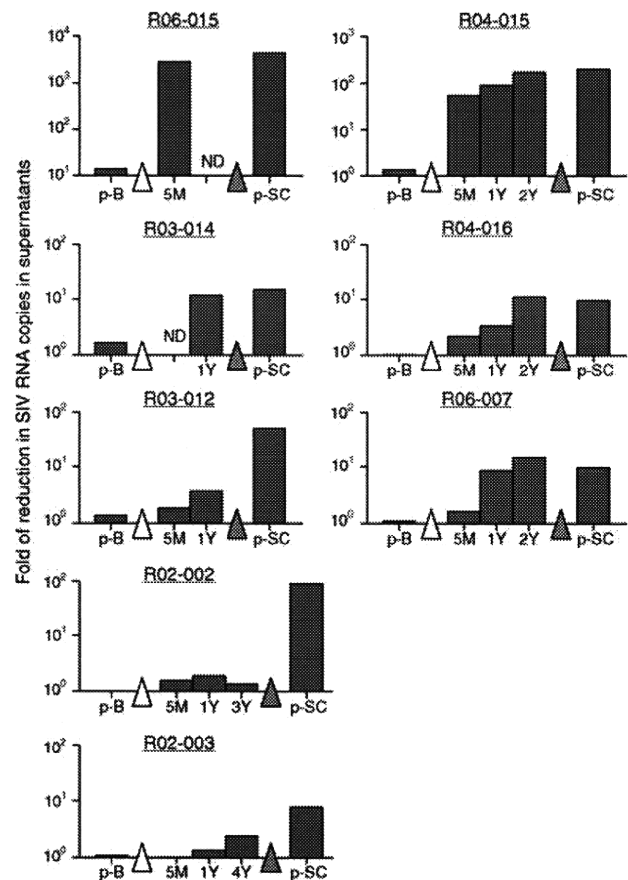


Fig. 3. Anti-SIV-G64723mt efficacy *in vitro* of CD8⁺ cells in simian immunodeficiency virus controllers. PBMC-derived CD8⁺ cells infected with SIV-G64723mt were cultured alone or cocultured with autologous PBMC-derived CD8⁺ cells at several time points at an *E:T* ratio of 1:4. The ratios of viral RNA levels in the supernatants from the coculture to those without CD8⁺ cells are shown. ND: not determined. p-B: 1 week after boost; 5M, 1Y, 2Y, 3Y, and 4Y: 5 months, 1, 2, 3, and 4 years after challenge, respectively; p-SC: 1 or 2 months after superchallenge. Open triangles indicate the time points of SIVmac239 challenge and closed triangles SIV-G64723mt superchallenge. PBMC, peripheral blood mononuclear cell; SIV, simian immunodeficiency virus.

two-fold reduction in viral production) of CD8⁺ cells, sooner or later, in the chronic phase. The levels of *in-vitro* anti-SIV-G64723mt efficacy of CD8⁺ cells tended to become higher in the chronic phase. Anti-SIVmac239 efficacy of CD8⁺ cells was not associated with anti-SIV-G64723mt efficacy. For instance, some CD8⁺ cells efficiently suppressed SIV-G64723mt but not SIVmac239 replication. After all, all SIV controllers acquired CD8⁺ cells able to suppress the mutant SIV-G64723mt replication *in vitro* in the chronic phase.

Control of a mutant simian immunodeficiency virus superchallenge

These animals were superchallenged with a mutant SIV, SIV-G64723mt, that has five *gag* mutations resulting in

escape from recognition by Gag₂₀₆₋₂₁₆-specific, Gag₂₄₁₋₂₄₉-specific, and Gag₃₆₇₋₃₈₁-specific CTLs around 1 year (R06-015, R03-014, and R03-012), 2 years (R04-015, R04-016, and R06-007), 3 years (R02-002), or 4 years (R02-003) after SIVmac239 challenge. The replicative ability of SIV-G64723mt is significantly lower than that of wild-type SIVmac239, but SIV-G64723mt challenge of naive 90-120-Ia-negative rhesus macaques can result in persistent viral replication and AIDS progression [23,28]. It has previously been shown that 90-120-Ia-positive macaques vaccinated with DNA-prime/SeV-Gag-boost are unable to contain a SIV-G64723mt challenge, whereas they can control replication of wild-type SIVmac239 [24]. Indeed, we confirmed that CD8⁺ cells obtained from these 90-120-Ia-positive vaccinees before challenge efficiently suppressed wild-type SIVmac239 but not SIV-G64723mt replication *in vitro*. In the present study, however, all eight wild-type SIV controllers contained the SIV-G64723mt superchallenge without detectable viremia (Fig. 1b). SIVmac239-specific neutralizing antibody responses were undetectable around the superchallenge in any of these controllers (Fig. 1a). These results indicate that, after SIVmac239 challenge, the SIV controllers acquired the potential to control SIV-G64723mt replication in the absence of neutralizing antibody responses, although to what extent CD8⁺ cell responses may contribute to this containment of SIV-G64723mt superchallenge remains unclear. Postsuperchallenge CD8⁺ cells suppressed both SIVmac239 and SIV-G64723mt replication *in vitro* efficiently (Figs. 2 and 3).

Simian immunodeficiency virus Gag-specific cytotoxic T lymphocyte responses in simian immunodeficiency virus controllers

Then, in these SIV controllers, we examined Gag₂₀₆₋₂₁₆-specific, Gag₂₄₁₋₂₄₉-specific, and Gag₃₆₇₋₃₈₁-specific CTL responses, which have previously been indicated responsible for control of SIVmac239 replication in 90-120-Ia-positive vaccinees [24] (Fig. 4a). In DNA/SeV-Gag vaccinated animals (R06-015, R03-014, R03-012, and R02-002), SIV-specific CTL responses were undetectable before SeV-Gag boost (data not shown), but Gag₂₀₆₋₂₁₆-specific, Gag₂₄₁₋₂₄₉-specific, and Gag₃₆₇₋₃₈₁-specific responses were efficiently induced 1 week after the boost. After SIVmac239 challenge, these animals showed efficient responses of these CTLs in the acute phase. These CTL levels were reduced in the chronic phase, but Gag₂₄₁₋₂₄₉-specific CTL responses were detectable even 1 year after challenge. In macaque R04-015 vaccinated with DNA/SeV-Gag₂₀₂₋₂₁₆-EGFP and DNA/SeV-Gag₂₃₆₋₂₅₀-EGFP, Gag₂₀₆₋₂₁₆-specific CTL responses were induced dominantly 1 week after boost and 2 weeks after SIVmac239 challenge, whereas Gag₂₄₁₋₂₄₉-specific CTL responses were detected predominantly in the chronic phase. In macaques R04-016 and R06-007 vaccinated with DNA/SeV-Gag₂₃₆₋₂₅₀-EGFP, Gag₂₄₁₋₂₄₉-specific CTL responses were induced dominantly 1 week after boost and 2 weeks after SIVmac239 challenge and

were maintained in the chronic phase. No significant enhancement of these CTL responses was observed after SIV-G64723mt superchallenge.

We also examined Gag-specific CTL responses in SIV controllers at several time points by using a panel of overlapping peptides (Gag peptide pools 1–10) spanning the entire SIVmac239 Gag (Fig. 4b). Group I macaques vaccinated with DNA/SeV-Gag elicited CTL responses directed against not only Gag peptide pool 5 (including Gag₂₀₆₋₂₁₆ and Gag₂₄₁₋₂₄₉) and 7 (including Gag₃₆₇₋₃₈₁) but also other Gag peptide pools after boost and after challenge; some peptide pool-specific CTLs were diminished, whereas others appeared in the chronic phase. In contrast, group II macaques eliciting CTL responses directed against single Gag₂₀₆₋₂₁₆ (R04-015) or Gag₂₄₁₋₂₄₉ (R04-016 and R06-007) epitope after boost showed predominant Gag peptide pool 5-specific CTL responses after challenge and accumulated multiple Gag epitope-specific CTL responses in the chronic phase. These results indicate dynamics of postchallenge Gag-specific CTL responses in vaccine-based SIV controllers. After SIV-G64723mt superchallenge, changes in the pattern of Gag-specific CTL responses were observed in some animals.

Simian immunodeficiency virus non-Gag antigen-specific cytotoxic T lymphocyte responses in simian immunodeficiency virus controllers

Next, in SIV controllers, we examined CTL responses directed against SIV non-Gag antigens by using panels of overlapping peptides spanning the entire SIVmac239 antigens other than Gag (Fig. 5a). These SIV controllers showed SIV non-Gag-specific CTL responses from the early phase after challenge. After SIV-G64723mt superchallenge, broadening or changes in the pattern of these CTL responses were observed in some animals; Vif-specific or Nef-specific CTL responses were detected predominantly, although we did not find common CTL epitopes in Vif or Nef.

Correlation of antigen-specific cytotoxic T lymphocyte levels with in-vitro antiviral efficacy levels

Finally, we analyzed correlation of antigen-specific CTL levels with in-vitro anti-SIVmac239 or anti-SIV-G64723mt efficacy levels of CD8⁺ cells (Fig. 5b). We found a correlation of anti-SIVmac239 efficacy levels with Gag₂₀₆₋₂₁₆-specific and Gag₂₄₁₋₂₄₉-specific CTL levels but not with total Gag-specific CTL levels. The anti-SIVmac239 efficacy levels did not correlate with either Gag₂₀₆₋₂₁₆-specific or Gag₂₄₁₋₂₄₉-specific CTL levels alone (data not shown), although our previous study [25] indicated inverse correlation between peak plasma viral loads and the levels of Gag₂₄₁₋₂₄₉-specific CTLs dominantly induced in DNA/SeV-Gag₂₃₆₋₂₅₀-EGFP-vaccinated animals in the acute phase after

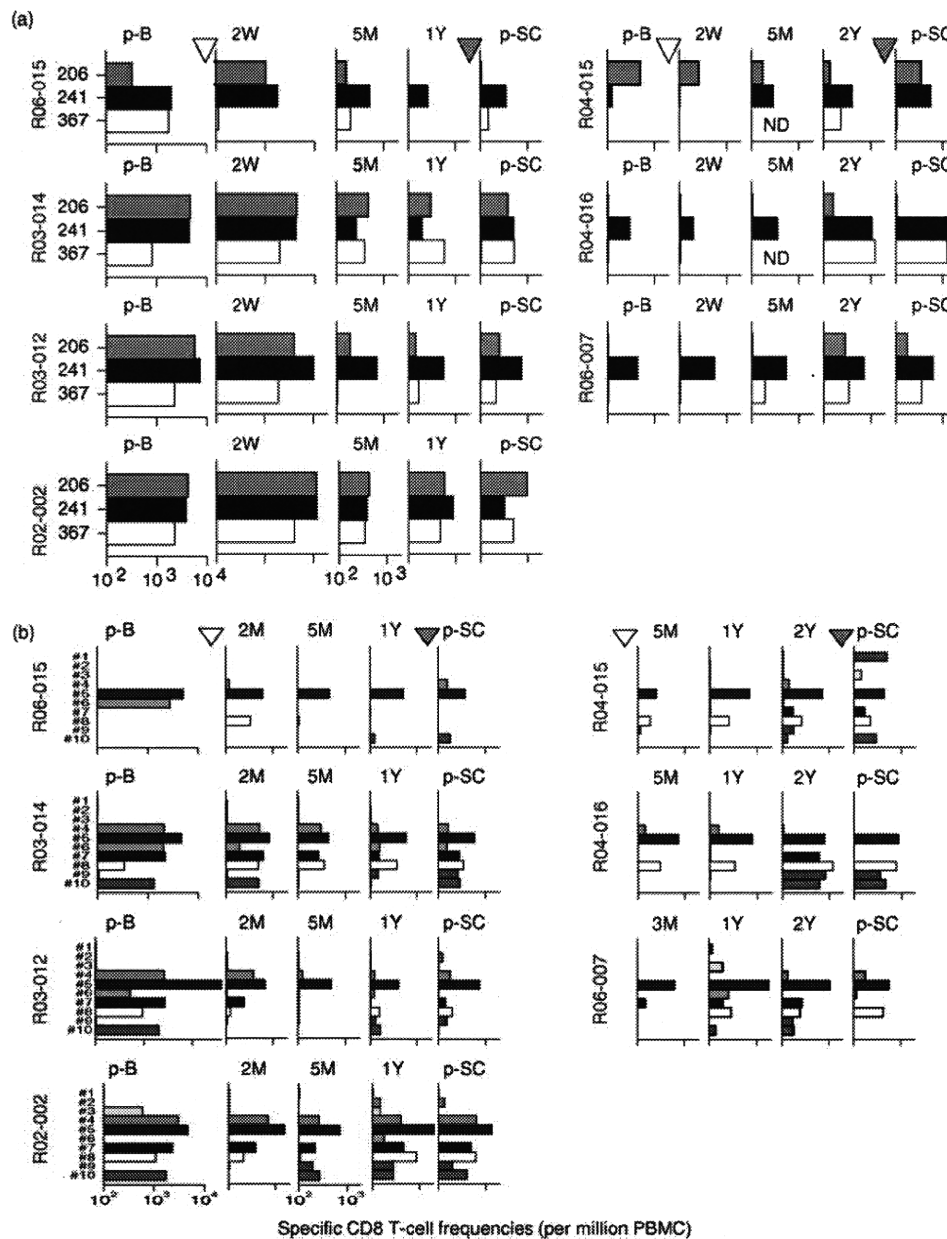


Fig. 4. Gag-specific CD8⁺ T-cell responses in simian immunodeficiency virus controllers. (a) Gag₂₀₆₋₂₁₆-specific (206), Gag₂₄₁₋₂₄₉-specific (241), and Gag₃₆₇₋₃₈₁-specific (367) CD8⁺ T-cell frequencies at several time points are shown. Regarding macaque R02-003, we confirmed efficient responses of these CTLs after boost and in the acute phase as reported previously [24] but did not have enough PBMC samples for the analyses in the chronic phase. (b) A panel of 117 overlapping peptides (15–17 amino acid in length and overlapping by 10–12 amino acid) spanning the entire SIV Gag amino acid sequence was divided into the following 10 pools (each consisting of 11 or 12 peptides): pool 1, first to 65th amino acid in SIV Gag; pool 2, 55th to 114th amino acid; pool 3, 104th to 165th amino acid; pool 4, 155th to 213th amino acid; pool 5, 202nd to 265th amino acid; pool 6, 255th to 316th amino acid; pool 7, 306th to 364th amino acid; pool 8, 354th to 416th amino acid; pool 9, 406th to 464th amino acid; and pool 10, 453rd to 510th amino acid. These Gag peptide pool-specific CD8⁺ T-cell frequencies at several time points are shown. ND: not determined. p-B: 1 week after boost; 2W, 5M, 1Y, and 2Y: 2 weeks, 5 months, 1, and 2 years after challenge, respectively; p-SC: 1 or 2 months after superchallenge. Open triangles indicate the time points of SIVmac239 challenge and closed triangles SIV-G64723mt superchallenge. CTL, cytotoxic T lymphocyte; PBMC, peripheral blood mononuclear cell; SIV, simian immunodeficiency virus.

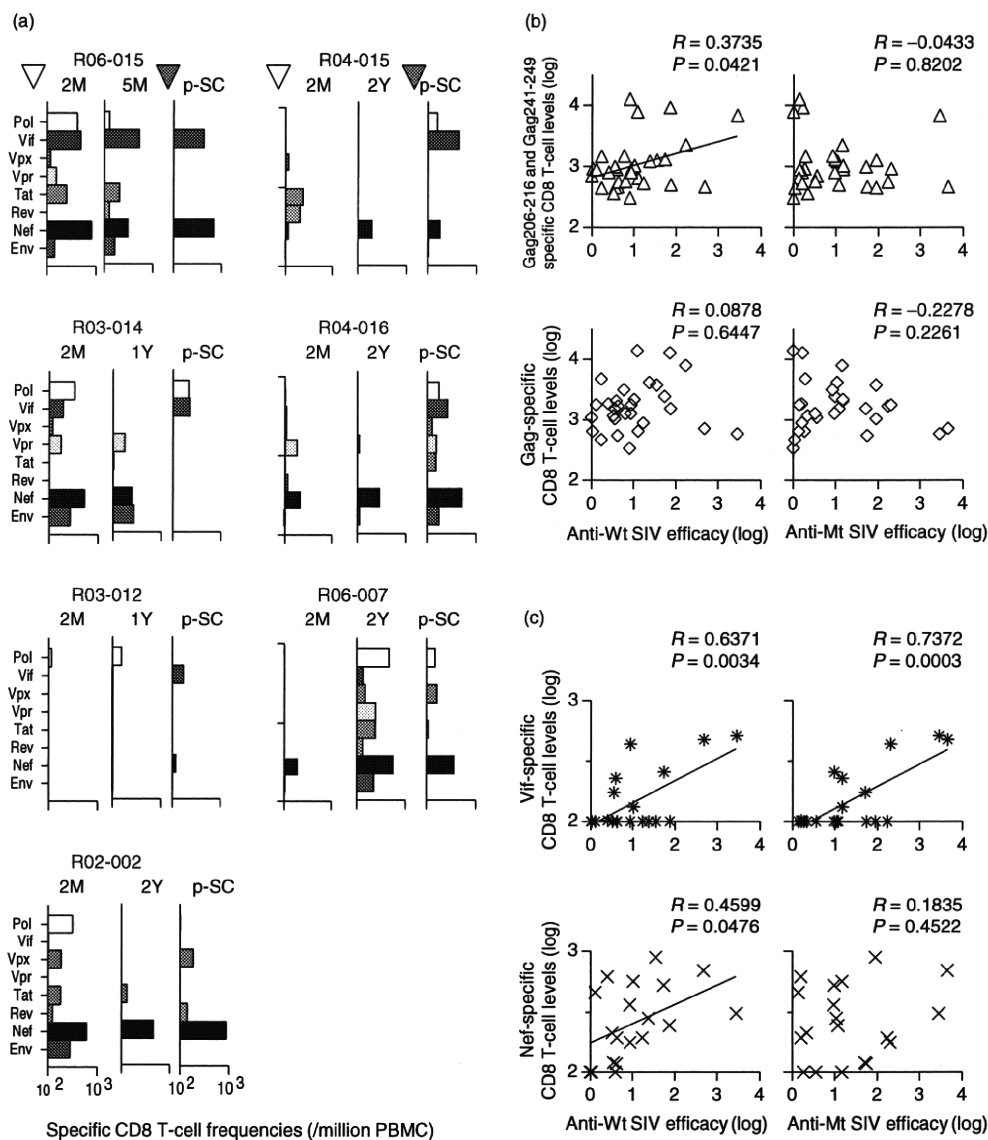


Fig. 5. Analysis of correlation between anti-SIVmac239 or anti-SIV-G64723mt efficacy *in vitro* and simian immunodeficiency virus antigen-specific CD8⁺ T-cell levels in simian immunodeficiency virus controllers. (a) SIV non-Gag antigen-specific CD8⁺ T-cell responses. Pol-specific, Vif-specific, Vpx-specific, Vpr-specific, Tat-specific, Rev-specific, Nef-specific, and Env-specific CD8⁺ T-cell frequencies at several time points were measured by using panels of overlapping peptides spanning the entire SIVmac239 Pol, Vif, Vpx, Vpr, Tat, Rev, Nef, and Env amino acid sequences, respectively. R02-003 PBMC samples were unavailable. 2M, 5M, 1Y, and 2Y: 2, 5 months, 1, and 2 years after challenge, respectively; p-SC: 1 or 2 months after superchallenge. Open triangles indicate the time points of SIVmac239 challenge and closed triangles SIV-G64723mt superchallenge. (b) Analysis of correlation between anti-SIVmac239 (Wt SIV) efficacy (left panels) or anti-SIV-G64723mt (Mt SIV) efficacy (right panels) levels and Gag₂₀₆₋₂₁₆-specific plus Gag₂₄₁₋₂₄₉-specific CTL (upper panels) or Gag-specific CTL (lower panels) levels ($n = 30$ in each panel). A correlation between anti-SIVmac239 efficacy levels and Gag₂₀₆₋₂₁₆-specific plus Gag₂₄₁₋₂₄₉-specific CTL levels is indicated ($P = 0.0421$, $R = 0.3735$). (c) Analysis of correlation between after challenge anti-SIVmac239 efficacy (left panels) or anti-SIV-G64723mt efficacy (right panels) levels and Vif-specific CTL (upper panels) or Nef-specific CTL (lower panels) levels ($n = 19$ in each panel). Correlations of anti-SIVmac239 efficacy levels with Vif-specific CTL ($P = 0.0034$, $R = 0.6731$) and with Nef-specific CTL levels ($P = 0.0476$, $R = 0.4599$) and a strong correlation between anti-SIV-G64723mt efficacy levels and Vif-specific CTL levels ($P = 0.0003$, $R = 0.7372$) are indicated. CTL, cytotoxic T lymphocyte; SIV, simian immunodeficiency virus.

challenge. Correlations of anti-SIVmac239 efficacy levels after challenge with Vif-specific CTL levels and with Nef-specific CTL levels were indicated. On the contrary,

anti-SIV-G64723mt efficacy levels after challenge strongly correlated with Vif-specific CTL levels, although any correlation of these levels with other SIV antigen-